WMO Statement on the State of the Global Climate in 2017

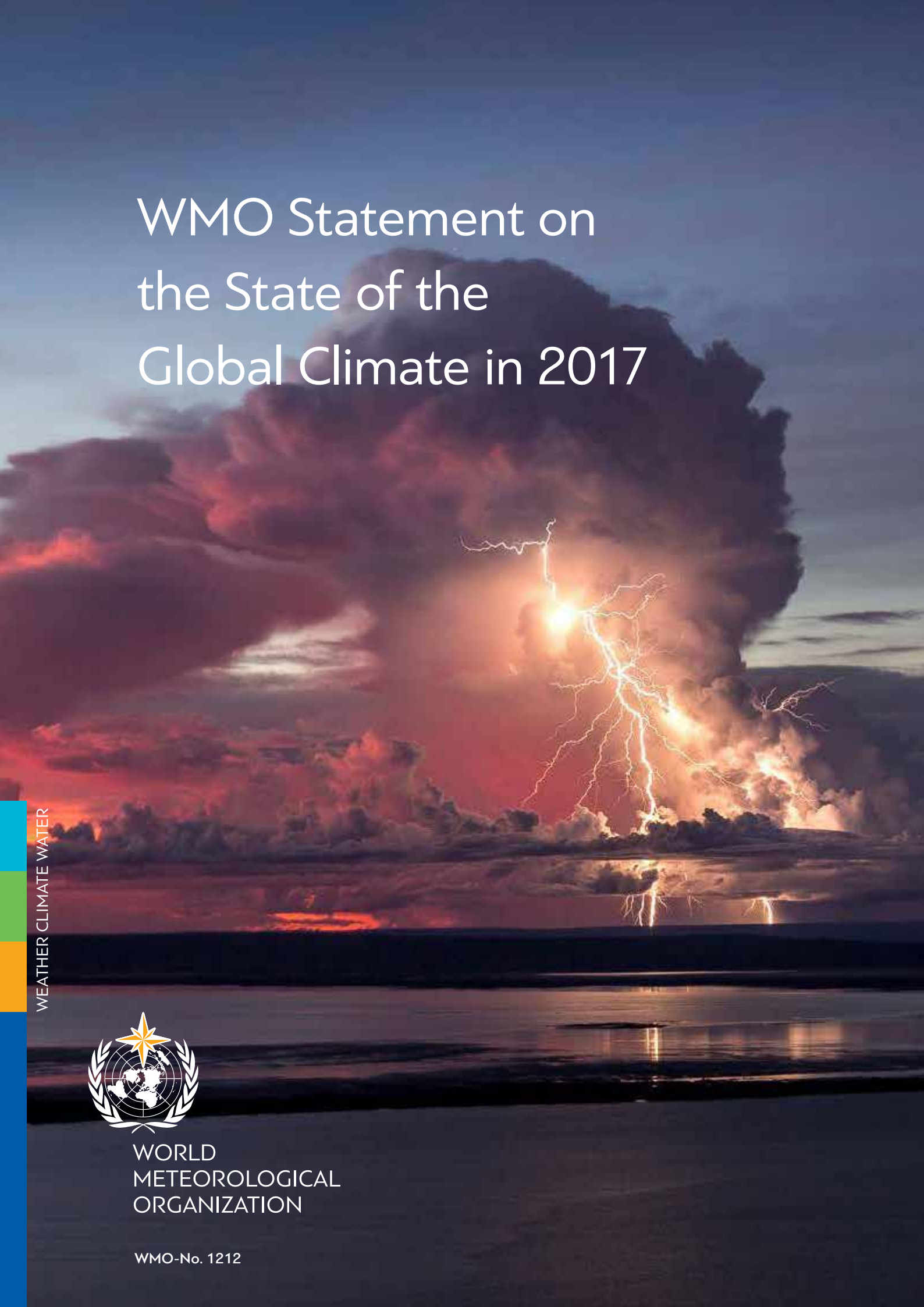

WEATHER CLIMATE WATER

WORLD METEOROLOGICAL ORGANIZATION

WMO-No. 1212

WMO-No. 1212

Chairperson, Publications Board
World Meteorological Organization (WMO)
7 bis, avenue de la Paix
P.O. Box 2300
CH-1211 Geneva 2, Switzerland

Tel.: +41 (0) 22 730 84 03
Fax: +41 (0) 22 730 81 17
Email: publications@wmo.int

ISBN 978-92-63-11212-5

This publication was issued in collaboration with the African Center of Meteorological Applications for Development (ACMAD), Niger; Regional Climate Centre for the Southern South American Region (RCC-SSA); European Centre for Medium-Range Weather Forecasts (ECMWF), United Kingdom of Great Britain and Northern Ireland; Japan Meteorological Agency (JMA); Met Office Hadley Centre, United Kingdom; Climatic Research Unit (CRU), University of East Anglia, United Kingdom; Climate Prediction Center (CPC); the National Centers for Environmental Information (NCEI) and the National Hurricane Center (NHC) of the National Oceanic and Atmospheric Administration (NOAA), United States of America; National Aeronautics and Space Administration, Goddard Institute for Space Studies (NASA GISS), United States; Global Precipitation Climatology Centre (GPCC), Germany; National Snow and Ice Data Center (NSIDC), United States; Commonwealth Scientific and Industrial Research Organization (CSIRO) Marine and Atmospheric Research, Australia; Global Snow Lab, Rutgers University, United States; Regional Climate Centre for Regional Association VI, Climate Monitoring, Germany; Beijing Climate Centre, China; Tokyo Climate Centre, Japan; International Research Centre on El Niño (CIIFEN), Ecuador; Caribbean Institute for Meteorology and Hydrology, Bridgetown, Barbados; Royal Netherlands Meteorological Institute (KNMI), Netherlands; Institute on Global Climate and Ecology (IGCE), Russian Federation; All-Russia Research Institute for Hydrometeorological Information-World Data Center (ARIHMI-WDC), Russian Federation; Global Atmospheric Watch Station Information System (GAWSIS), MeteoSwiss, Switzerland; World Data Centre for Greenhouse Gases (WDCGG), Japan Meteorological Agency, Japan; World Glacier Monitoring Service (WGMS), Switzerland; World Ozone and UV Radiation Data Centre (WOUDC), Environment and Climate Change, Canada; Niger Basin Authority, Niger. Other contributors are the National Meteorological and Hydrological Services or equivalent of: Algeria, Argentina, Australia, Austria, Bangladesh, Belarus, Belgium, Bosnia and Herzegovina, Brazil, Bulgaria, Canada, Chile, China, Colombia, Costa Rica, Croatia, Cuba, Cyprus, Czechia, Denmark, Ecuador, Estonia, Fiji, Finland, France, Gambia, Georgia, Germany, Greece, Hungary, Iceland, India, Indonesia, Iran, Islamic Republic of, Ireland, Israel, Italy, Japan, Kenya, Latvia, Lithuania, Luxembourg, Malaysia, Mali, Malta, Mauritius, Mexico, Morocco, Netherlands, New Zealand, Nigeria, Norway, Oman, Pakistan, Paraguay, Peru, Philippines, Portugal, Republic of Korea, Republic of Moldova, Romania, Russian Federation, Serbia, Singapore, Slovakia, Slovenia, South Africa, Spain, Sweden, Switzerland, Thailand, The former Yugoslav Republic of Macedonia, Tunisia, Turkey, Turkmenistan, Ukraine, United Arab Emirates, United Kingdom, United Republic of Tanzania, United States, Uruguay.

Various international organizations and national institutions contributed to this publication, including the Food and Agriculture Organization of the United Nations (FAO); Intergovernmental Oceanographic Commission of the United Nations Educational, Scientific and Cultural Organization (UNESCO); International Monetary Fund (IMF); International Organization for Migration (IOM); United Nations High Commissioner for Refugees (UNHCR); United Nations Office for Disaster Risk Reduction (UNISDR); United Nations Office for the Coordination of Humanitarian Affairs (OCHA), World Food Programme (WFP); World Health Organization (WHO); the Catholic University of Leuven, Belgium; the Centre for Research on the Epidemiology of Disasters (CRED); and Munich Re.

Cover illustration: Landi Bradshaw Photography

Contents

Foreword **3**

Executive summary **4**

Key climate indicators **5**

Temperature 5

Greenhouse gases 7

The Global Carbon Budget 10

The oceans in 2017 11

The cryosphere in 2017 13

Major drivers of interannual climate variability in 2017 15

Precipitation in 2017. 16

Extreme events 17

Climate risks and related impacts **29**

Agriculture and food security 29

Health 32

Population displacement 32

Economic impacts. 33

Vector-borne diseases: Zika in the Americas 34


GREENHOUSE GAS CONCENTRATIONS CONTINUE RISING
2017: WARMEST NON-EL NIÑO YEAR
2013–2017: WARMEST 5 YEARS ON RECORD
GLOBAL OCEAN HEAT CONTENT AT RECORD LEVELS
SEA-LEVEL RISE CONTINUES
State of the Global Climate 2017
OCEAN ACIDIFICATION CONTINUES
ARCTIC AND ANTARCTIC SEA ICE WELL BELOW AVERAGE
+41 MILLION AFFECTED BY FLOODS IN SOUTH ASIA
United Nations Office for the Coordination of Humanitarian Affairs
AGRICULTURE ACCOUNTED FOR ≈26% OF DAMAGES AND LOSSES ASSOCIATED WITH CLIMATE-RELATED DISASTERS
Food and Agriculture Organization of the United Nations
2ND YEAR OF MAJOR BLEACHING IN THE GREAT BARRIER REEF
≈30% OF THE WORLD'S POPULATION FACES EXTREME HEATWAVES
World Health Organization
Climate risks, extreme events and related impacts 2017
EXCEPTIONALLY HEAVY RAINS TRIGGERED DEADLY LANDSLIDES IN SIERRA LEONE AND COLOMBIA
+892 000 DROUGHT RELATED INTERNAL DISPLACEMENTS IN SOMALIA
United Nations High Commissioner for Refugees
MOST COSTLY HURRICANE SEASON ON RECORD
DESTRUCTIVE WILDFIRES AROUND THE WORLD

Foreword

For the past 25 years, the World Meteorological Organization (WMO) has published an annual Statement on the State of the Global Climate in order to provide authoritative scientific information about the global climate and significant weather and climate events occurring around the world. As we mark the 25th anniversary, and following the entry into force of the Paris Agreement, the importance of the information contained in the WMO Statement is greater than ever. WMO will continue working to increase the relevance of the information it provides to the Parties to the United Nations Framework Convention on Climate Change through this Statement and the annual WMO Greenhouse Gas Bulletin. These publications complement the assessment reports that the Intergovernmental Panel on Climate Change (IPCC) produces every six to seven years.

Since the inaugural Statement on the State of the Global Climate, in 1993, scientific understanding of our complex climate system has progressed rapidly. This is particularly true with respect to our understanding of mankind's contribution to climate change, and the nature and degree of such change. This includes our ability to document the occurrence of extreme weather and climate events and the degree to which they can be attributed to human influences on the climate.

In the past quarter of a century, atmospheric concentrations of carbon dioxide – whose rising emissions, along with those of other greenhouse gases, are driving anthropogenic climate change – have risen from 360 parts per million (ppm) to more than 400 ppm. They will remain above that level for generations to come, committing our planet to a warmer future, with more weather, climate and water extremes. Climate change is also increasingly manifested in sea level rise, ocean acidification and heat, melting sea ice and other climate indicators.

The global mean temperature in 2017 was approximately 1.1 °C above the pre-industrial era, more than half way towards the maximum limit of temperature increase of 2 °C sought through the Paris Agreement, which further strives to limit the increase to 1.5 °C above pre-industrial levels. The year 2017 was the warmest on record without an El Niño event, and one of the three warmest years behind the record-setting 2016. The world's nine warmest years have all occurred since 2005, and the five warmest since 2010.

Extreme weather claimed lives and destroyed livelihoods in many countries in 2017. Fuelled by warm sea-surface temperatures, the North Atlantic hurricane season was the costliest ever for the United States, and eradicated decades of development gains in small islands in the Caribbean such as Dominica. Floods uprooted millions of people on the Indian subcontinent, whilst drought is exacerbating poverty and increasing migration pressures in the Horn of Africa. It is no surprise that extreme weather events are identified as the most prominent risk facing humanity in the World Economic Forum's *Global Risks Report 2018*.

Because the societal and economic impacts of climate change have become so severe, WMO has partnered with other United Nations organizations to include information in the Statement on how climate has affected migration patterns, food security, health and other sectors. Such impacts disproportionately affect vulnerable nations, as evidenced in a recent study by the International Monetary Fund, which warned that a 1 °C increase in temperature would cut significantly economic growth rates in many low-income countries.

I would like to take this opportunity to express my gratitude to the National Meteorological and Hydrological Services of WMO Members, international and regional data centres and agencies, and climate experts from around the world for their contributions, and to United Nations sister agencies for their valuable input on societal and economic impacts. They have greatly assisted in ensuring that this annual Statement achieves the highest scientific standards and societal relevance and informs action on the Paris Agreement, the Sendai Framework for Disaster Risk Reduction and the United Nations Sustainable Development Goals.

(P. Taalas)
Secretary-General

Executive summary

Global mean temperatures in 2017 were 1.1 °C ± 0.1 °C above pre-industrial levels. Whilst 2017 was a cooler year than the record-setting 2016, it was still one of the three warmest years on record, and the warmest not influenced by an El Niño event. The average global temperature for 2013–2017 is close to 1 °C above that for 1850–1900 and is also the highest five-year average on record. The world also continued to see rising sea levels, with some acceleration, and increasing concentrations of greenhouse gases. The cryosphere continued its contraction, with Arctic and Antarctic sea ice shrinking.

The overall risk of heat-related illness or death has climbed steadily since 1980, with around 30% of the world's population now living in climatic conditions that deliver deadly temperatures at least 20 days a year.

There were many significant weather and climate events in 2017, including a very active North Atlantic hurricane season, major monsoon floods in the Indian subcontinent, and continuing severe drought in parts of east Africa. This contributed to 2017 being the year with the highest documented economic losses associated with severe weather and climate events. Extreme weather events continue to be rated by the World Economic Forum as amongst the most significant risks facing humanity, both in terms of likelihood and impact.[1]

Massive internal displacement in the context of drought and food insecurity continues across Somalia. From November 2016 to December 2017, 892 000 drought-related displacements were recorded by the United Nations High Commissioner for Refugees (UNHCR).

In August and September 2017, the three major and devastating hurricanes that made landfall in the southern United States and in several Caribbean islands in rapid succession broke modern records for such weather extremes and for loss and damage.

The information used in this report is sourced from a large number of National Meteorological and Hydrological Services (NMHSs) and associated institutions, as well as Regional Climate Centres, the World Climate Research Programme (WCRP), the Global Atmosphere Watch (GAW) and Global Cryosphere Watch (GCW). Information has also been supplied by a number of other international organizations, including the Food and Agriculture Organization of the United Nations (FAO), the World Food Programme (WFP), the World Health Organization (WHO), the United Nations High Commissioner for Refugees (UNHCR), the International Organization for Migration (IOM), the International Monetary Fund (IMF), the United Nations International Strategy for Disaster Reduction (UNISDR) and the Intergovernmental Oceanographic Commission of the United Nations Educational, Scientific and Cultural Organization (IOC-UNESCO).

Values of key climate indicators

Indicator	*Time period*	*Value*	*Ranking*
Global mean surface-temperature anomaly (1981–2010 baseline)	2017, annual mean	+0.46°C	Second-highest on record
Global ocean heat content change, 0–700 metre layer	2017, annual mean	1.581 x 1023 J	Highest on record
Global mean CO_2 surface mole fraction	2016, annual mean	403.3 parts per million	Highest on record
Global mean sea-level change since 1993	2017, December	8.0 cm	Highest on record
Arctic sea-ice extent summer minimum	2017, September	4.64 million km^2	Eighth-lowest on record

[1] World Economic Forum, 2018: *The Global Risks Report 2018*.

Key climate indicators

TEMPERATURE

The year 2017 was one of the world's three warmest years on record. A combination of five datasets, three of them using conventional surface observations and two of them reanalyses,[2] shows that global mean temperatures were 0.46 °C ± 0.1 °C above the 1981–2010 average,[3] and about 1.1 °C ± 0.1 °C above pre-industrial levels.[4] By this measure, 2017 and 2015 were effectively indistinguishable as the world's second and third warmest years on record, ranking only behind 2016, which was 0.56 °C above the 1981–2010 average. The years 2015, 2016 and 2017 were clearly warmer than any year prior to 2015, with all pre-2015 years being at least 0.15 °C cooler than 2015, 2016 or 2017.

The world's nine warmest years have all occurred since 2005, and the five warmest since 2010, whilst even the coolest year of the 21st century – 2008, 0.09 °C above the 1981–2010 average – would have ranked as the second-warmest year of the 20th century.

The five-year mean temperature for 2013–2017, 0.4 °C above the 1981–2010 average (and 1.0 °C above pre-industrial values), is also the highest on record. A five-year average gives a longer-term perspective on recent global temperatures whilst being less influenced than annual temperatures by year-to-year fluctuations such as those associated with the El Niño/Southern Oscillation (ENSO).

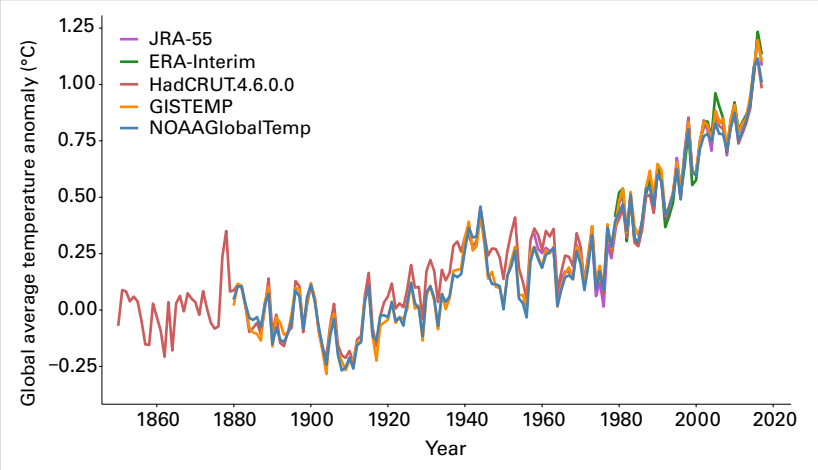

Figure 1. Global mean temperature anomalies, with respect to the 1850–1900 baseline, for the five global datasets *(Source: UK Met Office Hadley Centre)*

In the individual datasets, 2017 was second-warmest in the two reanalysis datasets (ERA-Interim and JRA-55) and in the dataset from the US National Aeronautics and Space Administration (NASA), and third-warmest in the datasets from the US National Oceanic and Atmospheric Administration (NOAA) and the UK Met Office Hadley Centre/Climatic Research Unit (CRU). Differences between individual datasets primarily relate to different ways in which they analyse data-sparse areas, especially in the Arctic which has experienced some of the world's strongest warming in recent years.

Global temperatures were well above average throughout the year. The strongest anomalies were early in the year, with each of the months from January to March being at least 0.5 °C above the 1981–2010 average, and March 0.64 °C above. For the remainder of the

The world's warmest years on record

Year	*Anomaly in respect of the 1981–2010 average (°C)*
2016	+0.56
2017	+0.46
2015	+0.45
2014	+0.30
2010	+0.28
2005	+0.27
2013	+0.24
2006	+0.22
2009	+0.21
1998	+0.21

[2] The conventional datasets used are those produced by the US National Oceanic and Atmospheric Administration (NOAA); the US National Aeronautics and Space Administration (NASA); and the Met Office, Hadley Centre/Climatic Research Unit (CRU), University of East Anglia (United Kingdom). The two reanalysis datasets used are the ERA-Interim dataset, produced by the European Centre for Medium-Range Weather Forecasts (ECMWF), and the JRA-55 dataset, produced by the Japan Meteorological Agency (JMA).

[3] For purposes other than comparison of temperatures with pre-industrial levels, this report uses 1981–2010 as a standard baseline period, as this is the period for which the widest range of datasets (especially satellite-based datasets) is available.

[4] For the purposes of this report, 1850–1900 is used as the baseline for pre-industrial temperatures. There is no appreciable difference between the temperature change derived from this baseline and that derived from other baselines used historically, such as 1880–1900.

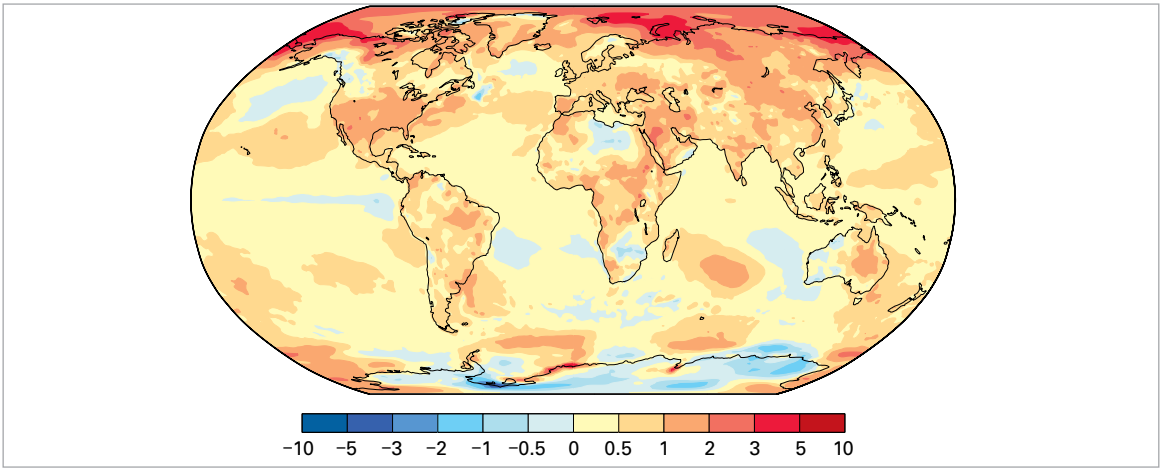

Figure 2. Surface-air temperature anomaly for 2017, with respect to the 1981-2010 average *(Source: ERA-Interim data, European Centre for Medium-range Weather Forecasts (ECMWF) Copernicus Climate Change Service)*

year, monthly global temperature anomalies were between 0.3 °C and 0.5 °C, the smallest monthly anomaly being 0.34 °C in June.

The year 2017 was clearly the warmest on record not influenced by an El Niño. Strong El Niño events, such as the one that occurred in 2015/2016, typically increase global mean temperatures by 0.1 °C to 0.2 °C in the year in which the event finishes, with a smaller increase in the event's first year. In the case of the 2015/2016 event, global temperatures were strongly boosted from October 2015 to April 2016, having a substantial influence on both the 2015 and 2016 annual values. Neutral ENSO conditions prevailed for most of 2017, with a weak La Niña developing late in the year.

Warmth in 2017 was notable for its spatial extent. The only land area of any size outside Antarctica that had annual mean temperatures in 2017 below the 1981–2010 average in conventional surface analyses was a section of western Canada centred on the interior of British Columbia. Reanalysis data also indicated some areas of below-average temperatures in parts of Africa where conventional data are sparse, including Libya and parts of the interior of southern Africa. Temperatures were 1 °C or more above average over most of the higher latitudes of Asia, including the Asian part of Russia, Mongolia and northern China. Other regions where 2017 temperatures were at least 1 °C above average included north-west Canada and Alaska, the southern half of the United States and parts of northern Mexico, and parts of eastern Australia. The largest anomalies, above 2 °C, were found at high northern latitudes, particularly in eastern Russia and north-west North America. Some coastal locations experiencing feedback from reduced sea-ice presence (such as Svalbard) were as much as 4 °C above average.

Despite the widespread high temperatures, only limited regions had their warmest year on record in 2017. Of 47 countries reporting mean temperatures at the national scale, only Argentina, Mauritius, Mexico, Spain and

Continental temperature anomalies

Region	*Anomaly in respect of the 1981–2010 average (°C)*	*2017 rank*	*Existing record*
North America	+0.84	6	+1.32 (2016)
South America	+0.54	2	+0.69 (2015)
Europe	+0.73	5	+1.18 (2014)
Africa	+0.54	4	+0.83 (2010)
Asia	+0.88	3	+0.92 (2015)
Oceania	+0.51	6	+0.73 (2013)

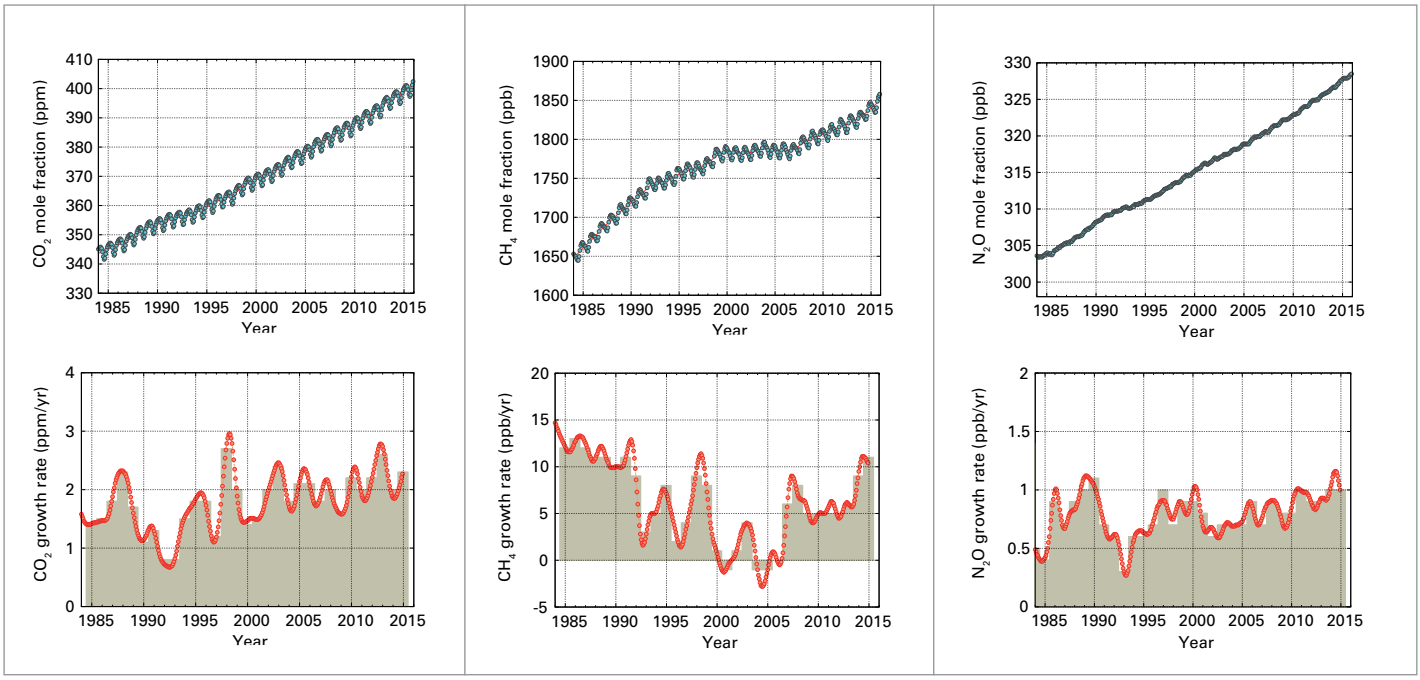

Uruguay had their warmest year on record. The Asian part of Russia also had its warmest year on record (the Russian Federation as a whole ranked fourth), as did five states in the southern half of the United States, and the eastern Australian states of New South Wales and Queensland.

All continents had one of their six warmest years on record in 2017, with South America ranking second, Asia third, Africa fourth, Europe fifth, and North America and Oceania sixth[5]. Temperatures in Africa were at record levels through mid-year, with monthly records set in May, June, July and September, but it cooled considerably from October onwards. South America had its second-warmest summer and second-warmest winter on record, whilst Oceania had its warmest July.

GREENHOUSE GASES

Increasing levels of greenhouse gases (GHGs) in the atmosphere are key drivers of climate change. Atmospheric concentrations are formed as a balance between emissions due to human activities and the net uptake from the biosphere and oceans. They are expressed in terms of dry mole fractions calculated from a global in-situ observational network for carbon dioxide (CO_2), methane (CH_4) and nitrous oxide (N_2O).

Global average figures for 2017 will not be available until late 2018. Real-time data from a number of specific locations, including Mauna Loa (Hawaii) and Cape Grim (Tasmania) indicate that levels of CO_2, CH_4 and N_2O continued to increase in 2017, but it is not yet clear how the rate of increase compares with that in 2016 or in previous years.

In 2016, GHG concentrations reached new highs with CO_2 at 403.3±0.1 parts per million (ppm), CH_4 at 1853±2 parts per billion (ppb) and N_2O at 328.9±0.1 ppb. These values constitute, respectively, 145%, 257% and 122% of pre-industrial (before 1750) levels.

The increase in CO_2 from 2015 to 2016 was larger than the increase observed from 2014 to 2015 and the average over the last decade, and it was the largest annual increase observed in the post-1984 period. The El Niño event contributed to the increased growth rate in 2016, both through higher emissions from terrestrial sources (e.g. forest fires) and decreased uptake of CO_2 by vegetation in drought-affected areas. The El Niño event in 2015/2016 contributed to the increased growth rate through complex two-way interactions between climate change and the carbon cycle.

Figure 3. Top row: Globally averaged mole fraction (measure of concentration), from 1984 to 2016, of CO_2 in parts per million (left), CH_4 in parts per billion (middle) and N_2O in parts per billion (right). The red line is the monthly mean mole fraction with the seasonal variations removed; the blue dots and line depict the monthly averages. Bottom row: The growth rates representing increases in successive annual means of mole fractions for CO_2 in parts per million per year (left), CH_4 in parts per billion per year (middle) and N_2O in part per billion per year (right). *(Source: WMO Global Atmosphere Watch)*

[5] Continental temperatures are as reported by NOAA, and are available at https://www.ncdc.noaa.gov/sotc/global-regions/201801.

PALEO AND CURRENT CONCENTRATIONS OF CO_2

The reconstruction of past climate provides an opportunity to learn how the Earth system responded to high concentrations of atmospheric carbon dioxide (CO_2). To obtain information about the state of the atmosphere before instrumental records began, combinations of proxies are used in which physical characteristics of past environmental conditions are preserved. Tiny bubbles of ancient air captured in ice cores when new snow accumulating at the top solidified into ice, can be directly measured and give some insight into the composition of the atmosphere in the past.

Direct measurements of atmospheric CO_2 over the past 800 000 years (see figure) provide proof that over the past eight swings between ice ages (glacials) and warm periods similar to today (interglacials) atmospheric CO_2 varied between 180 and 280 parts per million (ppm), demonstrating that today's CO_2 concentration of 400 ppm exceeds the natural variability seen over hundreds of thousands of years. Over the past decade, new high-resolution ice core records have been used to investigate how fast atmospheric CO_2 changed in the past. After the last ice age, some 23 000 years ago, CO_2 concentrations and temperature began to rise. During the period recorded in the West Antarctica ice core, fastest CO_2 increases (16 000, 15 000 and 12 000 years ago) ranged between 10 and 15 ppm over 100–200 years. In comparison, CO_2 has increased by 120 ppm in the last 150 years due to combustion of fossil fuel.

Periods of the past with a CO_2 concentration similar to the current one can provide estimates for the associated "equilibrium" climate. In the mid-Pliocene, 3–5 million years ago, the last time that the Earth's atmosphere contained 400 ppm of CO_2, global mean surface temperature was 2–3 °C warmer than today, the Greenland and West Antarctic ice sheets melted and even some of the East Antarctic ice was lost, leading to sea levels that were 10–20 m higher than they are today. During the mid-Miocene (15–17 million years ago), atmospheric CO_2 reached 400–650 ppm and global mean surface temperature was 3–4 °C warmer than today.

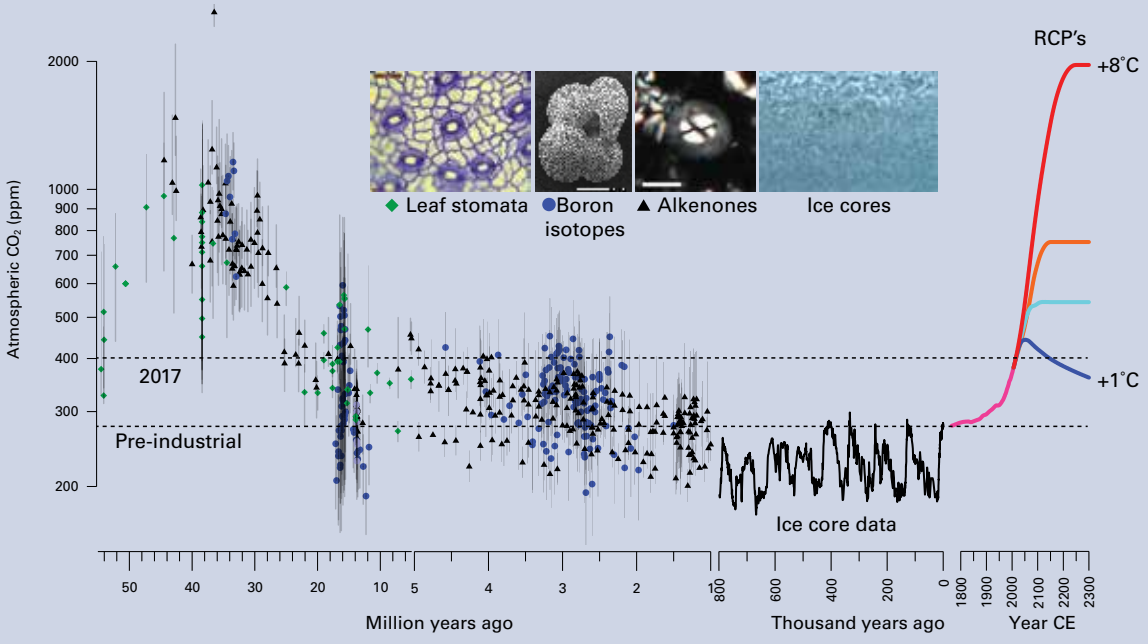

CE – Common Era

Reconstructions of atmospheric CO_2 over the past 55 million years are generated from proxy data that include boron isotopes (blue circles), alkenones (black triangles) and leaf stomata (green diamonds). Direct measurements from the past 800 000 years are acquired from Antarctic ice cores and modern instruments (pink). Future estimates include representative concentration pathways (RCPs) 8.5 (red), 6 (orange), 4.5 (light blue), and 2.6 (blue). References for all data shown in this plot are listed in the extended online version (http://www.wmo.int/pages/prog/arep/gaw/ghg/ghg-bulletin13).

For CH_4, the increase from 2015 to 2016 was slightly smaller than that observed from 2014 to 2015 but larger than the average over the past decade. For N_2O, the increase from 2015 to 2016 was also slightly smaller than that observed from 2014 to 2015 and lower than the average growth rate over the past 10 years.

OZONE

The 2017 Antarctic ozone hole was relatively small by the standards of recent decades. This largely reflects local atmospheric conditions in 2017 and is not, in itself, indicative of a more sustained downward trend. Most ozone hole indicators show weak, non-significant downward trends over the last 20 years.

The daily ozone hole area reached a maximum for the season of 19.6 million km² on 11 September. The first part of the season, up to the second week of September, saw the size of the Antarctic ozone hole at levels close to the 1979–2016 average. However, the polar vortex became unstable and elliptical in the third week of September, with temperatures at the polar cap (60–90°S) rising 5–7 °C above the long-term mean. This resulted in a rapid decrease in the size of the ozone hole before a small increase around the end of September.

The average area of the ozone hole through the peak of the season (from 7 September to 13 October) was 17.4 million km². This is the smallest value since 2002 (12.0 million km²) and also smaller than in 2012, the lowest value in the 2003–2016 period (17.8 million km²). The average ozone hole area over the 30 worst consecutive days was 17.5 million km². This is also the lowest value observed since 2002 (15.5 million km²) and again somewhat smaller than in 2012 (18.9 million km²).

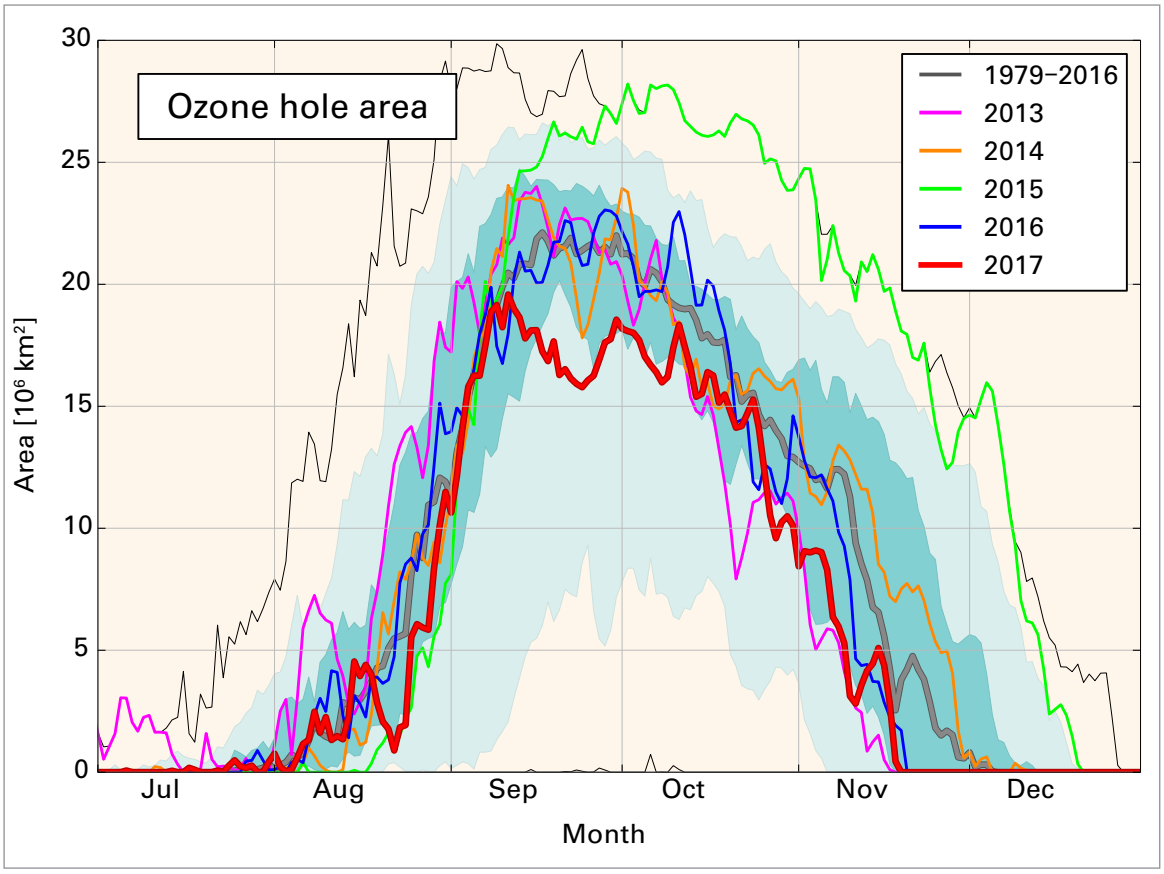

Figure 4. Area (millions of km²) where the total ozone column is less than 220 Dobson units. The year 2017 is shown in red. The most recent years are shown for comparison as indicated by the legend. The smooth, thick grey line is the 1979–2016 average. The dark green-blue shaded area represents the 30th to 70th percentiles and the light green-blue shaded area represents the 10th and 90th percentiles for the time period 1979–2016. The thin black lines show the maximum and minimum values for each day during the 1979–2016 period. The plot is made at WMO on the basis of data downloaded from the Ozone Watch website at the US National Aeronautics and Space Administration (NASA). The NASA data are based on satellite observations from the Ozone Mapping and Profiler Suite (OMPS), Ozone Monitoring Instruments (OMI) and the Total Ozone Mapping Spectrometer (TOMS).

The Global Carbon Budget

Josep G. Canadell,[1] Corinne Le Quéré,[2] Glen Peters,[3] Robbie Andrew,[3] Pierre Fridlingstein,[4] Robert B. Jackson,[5] Tatiana Ilyina[6]

Accurately assessing carbon dioxide (CO_2) emissions and redistribution within the atmosphere, oceans, and land – the "global carbon budget" – helps us capture how humans are changing the Earth's climate, supports the development of climate policies, and improves projections of future climate change.

Carbon dioxide emissions from fossil fuels and industry have been growing for decades with pauses only during global economic downturns. For the first time, emissions stalled from 2014 to 2016 while the global economy continued to expand. Nonetheless, CO_2 accumulated in the atmosphere at unprecedented rates close to 3 parts per million (ppm) per year in 2015 and 2016, despite stable fossil fuel emissions (figure, top). This surprising dynamic was caused by strong El Niño warming in 2015 and 2016, when the land CO_2 sink was less efficient in removing atmospheric CO_2, and emissions from fires were above average (in 2015). Preliminary data for 2017 show that emissions from fossil fuels and industry resumed growing at about 1.5% (0.7%–2.4%, leap year adjusted), from 36.2±2.0 billion tonnes of CO_2 in 2016 to a record high of 36.6±2.0 billion tonnes in 2017 – 65% higher than in 1990.

Carbon dioxide emissions from change in land use were 4.8±2.6 billion tonnes in 2016, accounting for 12% of all anthropogenic CO_2 emissions, and are expected to remain stable or slightly lower for 2017 on the basis of initial observations using satellite data. Together, land use change and fossil fuel emissions reached an estimated 41.5±4.4 billion tonnes of CO_2 in 2017.

Of all anthropogenic CO_2 emissions, only about 45% remained in the atmosphere on an annual average over the past decade: 25% were removed by the oceans and 30% were removed by the terrestrial biosphere (figure, bottom). However, due to the strong El Niño conditions, the increase from 2015 to 2016 in atmospheric CO_2 concentration was 22.1±0.7 billion tonnes (54% of total emissions; 2.85 ppm) which is larger than the average for 2007–2016. Ocean and terrestrial ecosystems removed 9.5±1.8 billion tonnes of CO_2 (23%) and 9.9±3.7 billion tonnes of CO_2 (24%), respectively.

There are substantial uncertainties in the quantification of the land and ocean carbon sinks on sub-decadal and decadal time scales, and in the reconstruction of cumulative emissions across centuries of the industrial era, particularly historical emissions from changes in land use.

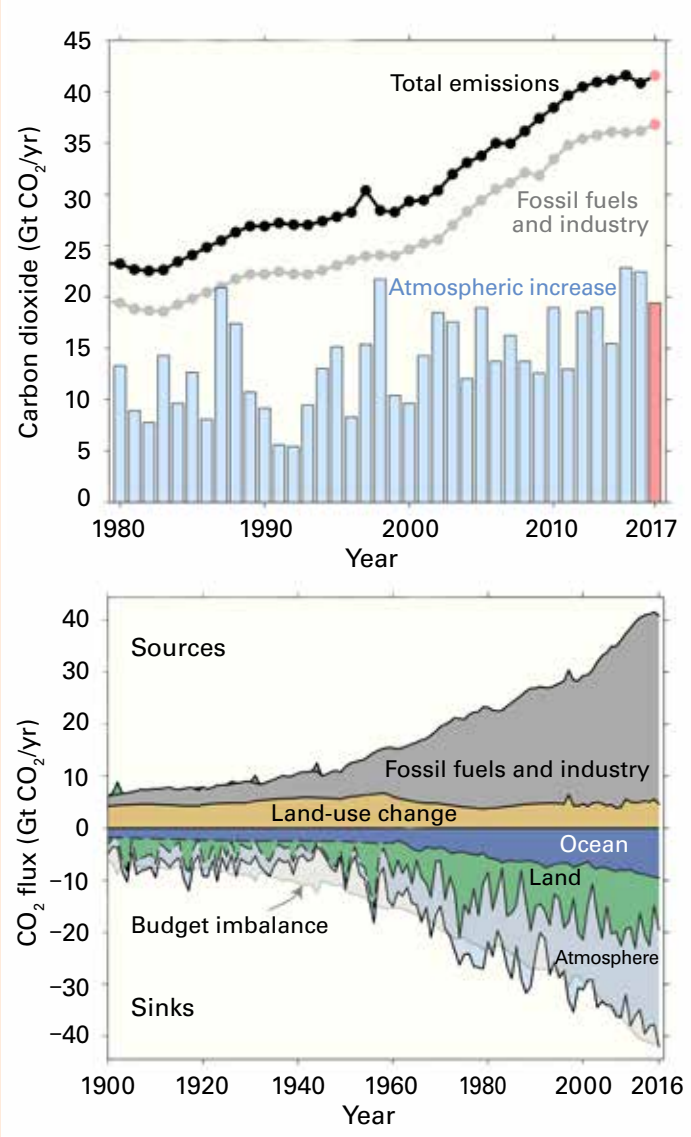

Trends in anthropogenic CO_2 emissions and growth of atmospheric CO_2, 1980–2017. Total emissions minus fossil fuel emissions equals emissions from change in land use (top). The historical global carbon budget, 1900–2016 (bottom) *(Source: Global Carbon Project, http://www.globalcarbonproject.org/carbonbudget; Le Quéré, C. et al., 2018: The Global Carbon Budget 2017.* Earth System Science Data, *10, 405–448); and March 2018 updates).*

[1] Global Carbon Project, Commonwealth Scientific and Industrial Research Organisation (CSIRO) Oceans and Atmosphere, Canberra, Australia

[2] Tyndall Centre for Climate Change Research, University of East Anglia, Norwich, United Kingdom

[3] Center for International Climate and Environmental Research (CICERO) – Oslo (CICERO), Oslo, Norway

[4] College of Engineering, Mathematics and Physical Sciences, University of Exeter, United Kingdom

[5] Department of Earth System Science, Woods Institute for the Environment and Precourt Institute for Energy, Stanford University, Stanford, United States

[6] Max Planck Institute for Meteorology, Hamburg, Germany

THE OCEANS IN 2017

TEMPERATURE

Global sea-surface temperatures in 2017 were somewhat below the levels of 2015 and 2016, but still ranked as the third warmest on record. The most significant sea-surface temperature anomalies were in the western tropical Pacific and the western and central subtropical South Indian Ocean. In both regions, sea-surface temperatures were widely 0.5 °C to 1.0 °C above the 1981–2010 average, locally exceeding 1.0 °C above average in the Indian Ocean, and were generally at record-high levels. In contrast, temperatures were slightly below average over most of the eastern Indian Ocean and over the central and eastern equatorial Pacific, the latter being consistent with weak La Niña conditions which developed late in the year. They were also slightly below average in parts of the far southern Atlantic. The area of cool waters in the north-east Atlantic south of Iceland was less prominent than in most recent years.

For the second successive year, above-average sea-surface temperatures off the east coast of Australia resulted in significant coral bleaching in the Great Barrier Reef, this time focused on central areas of the Reef rather than the northern areas affected in 2016.[6] Significant bleaching was also reported in other parts of the western tropical Pacific,[7] including Micronesia and Guam, although global bleaching was less extensive than it had been in 2016. Later in the year, exceptionally warm sea-surface temperatures (generally 2 °C or more above average, and 0.5 °C or more above previous records for the time of year) affected the southern Tasman Sea, coinciding with record high monthly temperatures in New Zealand (especially the South Island) and Tasmania. Whilst marine impacts of this event are still becoming apparent, there has already been a shift in the distribution of fish species, with snapper being caught off Fiordland (far south-west New Zealand) for the first time.

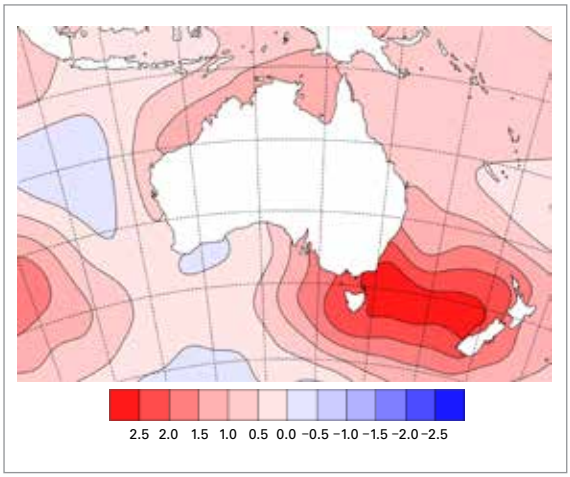

Figure 5. 5 December 2017 monthly sea-surface temperature anomalies (°C), showing temperatures 2.5°C or more above average in the southern Tasman Sea.
(Source: Australian Bureau of Meteorology)

Ocean heat content, a measure of the heat in the oceans through their upper layers, reached new record highs in 2017. Mean ocean heat content for 2017 for the 0–700 metre layer was 158.1 ZJ,[8] 6.9 ZJ higher than the previous annual mean record set in 2015. The mean for the October–December 2017 quarter, 163.4 ZJ, was also the highest quarterly value on record. The ocean heat content for the 0–2000 metre layer (233.5 ZJ) was also the highest on record, although records for this layer only extend back to 2005. Annual records for the 0–700 metre layer were also set for the northern hemisphere and for the Atlantic and Pacific Oceans, although the Indian Ocean had its lowest value since 2009.

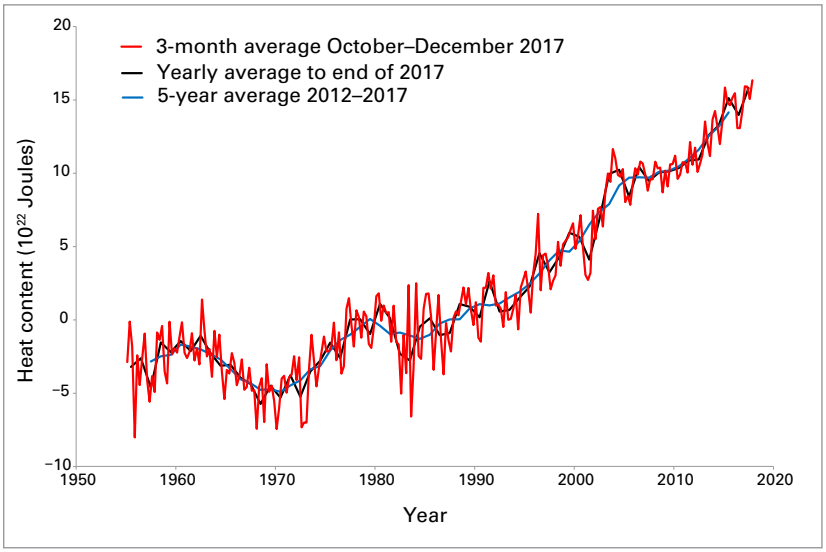

Figure 6. Global ocean heat content change (x 10^{22} J) for the 0–700 metre layer: three-monthly means (red), and annual (black) and 5-year (blue) running means, from the US National Oceanic and Atmospheric Administration (NOAA) dataset.
(Source: prepared by WMO using data from NOAA National Centers for Environmental Information)

[6] Australian Research Council (ARC) Centre of Excellence, Coral Reef Studies, https://www.coralcoe.org.au/.

[7] NOAA Coral Reef Watch, coralreefwatch.noaa.gov.

[8] Data sourced from NOAA; 1 ZJ (zetajoule) = 10^{21} J, a standard unit of energy.

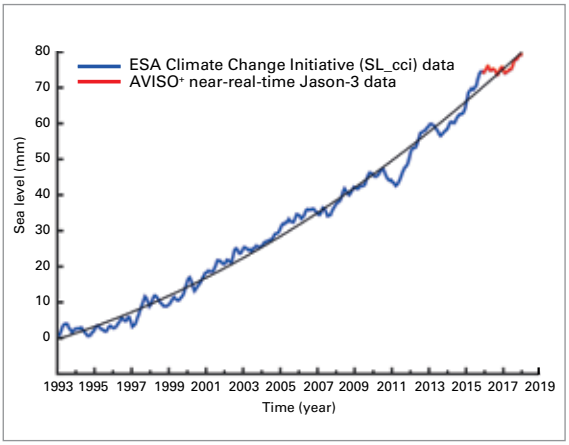

Figure 7. Global mean sea-level time series (with seasonal cycle removed), January 1993–January 2018, from satellite altimetry multi-missions. Data from AVISO *(Source: Collecte-Localisation-Satellite (CLS) – Laboratoire d'Etudes en Géophysique et Océanographie Spatiales (LEGOS))*

SEA LEVEL

The global mean sea level (GMSL) was relatively stable in 2016 and early 2017. This is because the temporary influence of the 2015/2016 El Niño (during which the GMSL peaked in early 2016 at around 10 millimetres above the 2004–2015 trend) continued to diminish and the GMSL reverted to values closer to the long-term trend. However, most recent sea-level data indicate that the GMSL has been rising again since mid-2017.

The pie charts show the contributions of individual components of the sea-level budget (expressed in percentage of the observed global mean sea level) for two periods, 1993–2004 and 2004–2015.[9] It clearly shows that the magnitude of almost all components has increased in recent years, particularly melting of the polar ice sheets, mostly in Greenland and to a lesser extent in Antarctica. Accelerated ice-mass loss from the ice sheets is the main cause of acceleration of the global mean sea-level rise, as revealed by satellite altimetry. This is even clearer when year-to-year fluctuations due to El Niño and La Niña as well as temporary cooling from the 1991 Mt Pinatubo eruption are removed.[10]

The bar chart (bottom) shows annual mean altimetry-based sea level (blue bars) and sum of thermal expansion and ocean mass component (red bars) for the years 2005 to 2016. Black vertical bars are associated uncertainties. Thermal expansion is based on Argo data[11] and ocean mass is derived from the Gravity Recovery and Climate Experiment (GRACE) (updates from Johnson and Chambers, 2013,[12] Lutchke et al., 2013,[13]

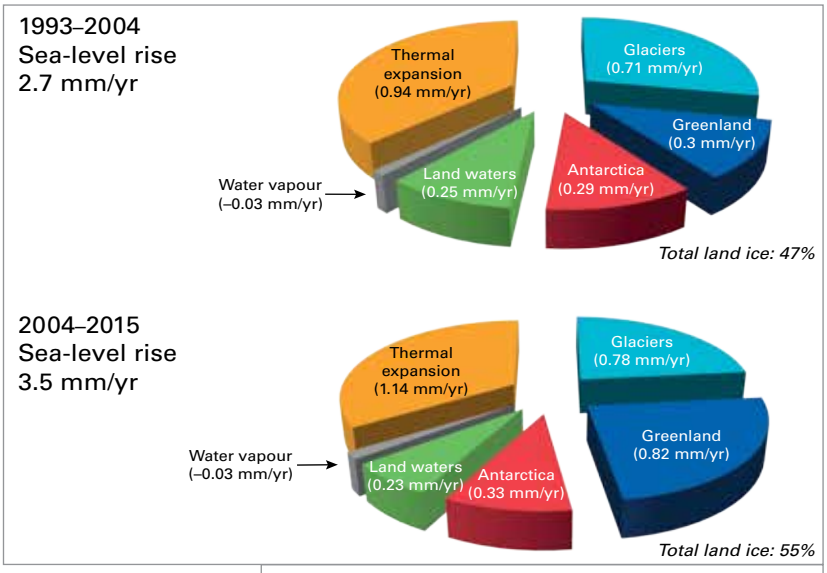

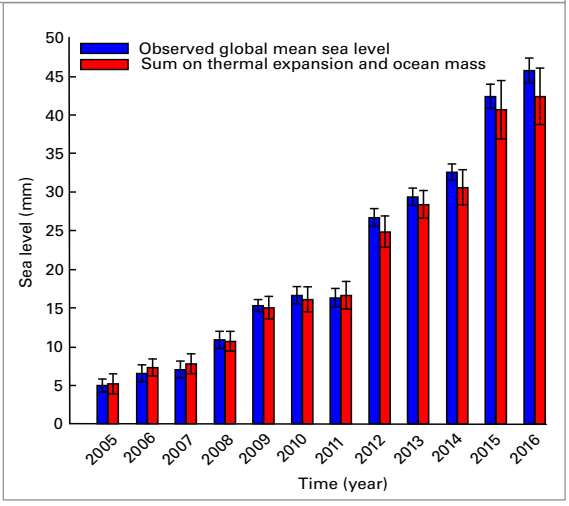

Figure 8. Percentage of individual contributions to global mean sea-level rise in 1993–2004 and 2004–2015 (top); annual sea-level budget (2005–2016) (bottom) *(Source: Dieng, H. et al., 2017: New estimate of the current rate of sea level rise from a sea level budget approach.* Geophysical Research Letters, *44)*

[9] Dieng, H. et al., 2017: New estimate of the current rate of sea level rise from a sea level budget approach. *Geophysical Research Letters*, 44, doi:10.1002/2017GL073308.

[10] Nerem, R.S. et al., 2018: Climate-change-driven accelerated sea-level rise detected in the altimeter era. *Proceedings of the National Academy of Sciences of the United States of America*, published on line on 13 February 2018.

[11] Ibid.

[12] Johnson, G. C. and D. P. Chambers, 2013: Ocean bottom pressure seasonal cycles and decadal trends from GRACE Release-05: Ocean circulation implications. *Journal of Geophysical Research*, Oceans, Vol.118, 9:4228–4240, doi: 10.1002/jgrc.20307.

[13] Luthcke, S. B. et al., 2013: Antarctica, Greenland and Gulf of Alaska land-ice evolution from an iterated GRACE global mascon solution. *Journal of Glaciology*, 59:613–631, doi:10.3189/2013JoG12J147.

Watkins et al., 2015[14]). The sea-level budget is almost closed (i.e. the observed change can be almost fully accounted for by the known changes in the contributing components) within respective error bars, although since 2012 the sum of contributions from thermal expansion and changes in ocean mass is generally slightly lower than the observed change in annual sea level. The plot also shows a clear increase of the mean sea level from one year to another.

OCEAN ACIDIFICATION

The ocean absorbs up to 30% of the annual emissions of anthropogenic CO_2 into the atmosphere, helping to alleviate the impacts of climate change on the planet. However, this comes at a steep ecological cost, as the absorbed CO_2 reacts in seawater and changes acidity levels in the ocean. More precisely, this involves a decrease in seawater pH together with closely linked shifts in the carbonate chemistry of the waters, including the saturation state of aragonite, which is the main form of calcium carbonate used by key species to form shells and skeletal material (e.g. reef-building corals and shelled molluscs). Observations of marine acidity in open ocean and coastal locations have revealed that present-day conditions are often outside pre-industrial bounds. In some regions, the changes are amplified by natural processes such as upwelling (where cold water that is rich in CO_2 and nutrients rises from the deep toward the sea surface), resulting in conditions outside biologically relevant thresholds.

Projections of future ocean conditions show that ocean acidification affects all areas of the ocean, while consequences for marine species, ecosystems and their functioning vary. Over the past 10 years, various studies have confirmed that ocean acidification is directly influencing the health of coral reefs; the success, quality and taste of aquaculture-raised fish and seafood; and the survival and calcification of several key organisms. These alterations often affect species at lower trophic levels and have cascading effects within the food web, which are expected to result in increasing impacts on coastal economies.

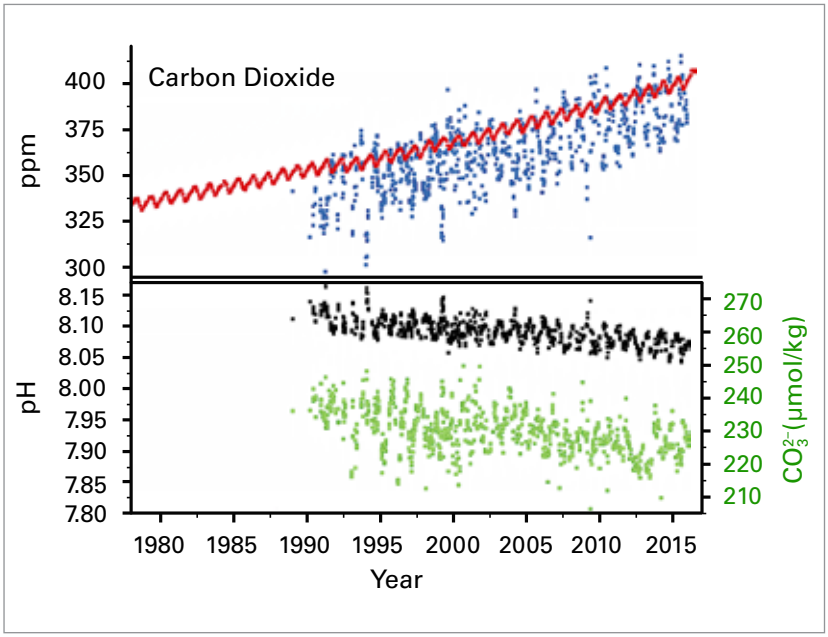

Figure 9. Trends in surface (< 50 m) ocean carbonate chemistry calculated from observations obtained at the Hawaii Ocean Time-series (HOT) Program in the North Pacific over 1988–2015. The upper panel shows the linked increase in atmospheric (red points) and seawater (blue points) CO_2 concentrations. The bottom panel shows a decline in seawater pH (black points, primary y-axis) and carbonate ion concentration (green points, secondary y-axis). Ocean chemistry data were obtained from the Hawaii Ocean Time-series Data Organization & Graphical System (HOT-DOGS). *(Source: US National Oceanic and Atmospheric Administration (NOAA), Jewett and Romanou, 2017)*

Further, ocean acidification does not impact marine ecosystems in isolation. Multiple other environmental stressors can interact with ocean acidification, such as ocean warming and stratification, de-oxygenation and extreme events, as well as other anthropogenic perturbations such as overfishing and pollution.

There has been a consistent trend in ocean acidification over time. Since records at Aloha station (north of Hawaii) began in the late 1980s, seawater pH has progressively fallen, from values above 8.10 in the early 1980s to between 8.04 and 8.09 in the last five years.

THE CRYOSPHERE IN 2017

Sea-ice extent was well below the 1981–2010 average throughout 2017 in both the Arctic and Antarctic. The winter maximum of Arctic sea ice of 14.42 million square kilometres, reached on 7 March, was the lowest winter maximum in the satellite record, 0.10 million square kilometres below the previous record low set in 2015. However, melting during the spring and summer was slower than in some recent years. The summer minimum of 4.64 million square kilometres on 13 September was the eighth-lowest on record, 1.25 million square kilometres above the 2012 record low. A slow

[14] Watkins, M. et al., 2015: Improved methods for observing Earth's time variable mass distribution with GRACE using spherical cap mascons. *Journal of Geophysical Research*, Solid Earth, 120:2648–2671, doi:10.1002/2014JB011547.

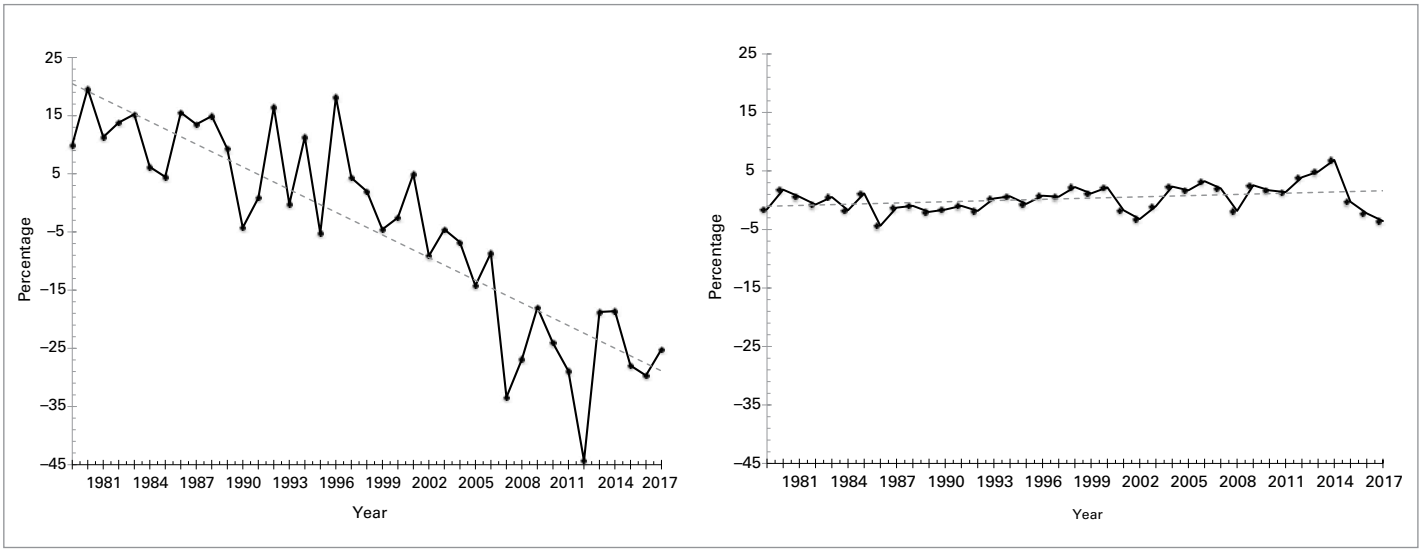

Figure 10. (left) September sea-ice extent for the Arctic, and (right) September sea-ice extent for the Antarctic. Percentage of long-term average of the reference period 1981–2010
(Source: prepared by WMO using data from the US National Snow and Ice Data Center)

freeze-up during the autumn saw Arctic sea-ice extent once again at near record low levels for the time of year by the end of December.

Antarctic sea-ice extent was at or near record low levels throughout the year. The summer minimum of 2.11 million square kilometres, recorded on 3 March, was 0.18 million square kilometres below the previous record set in 1997, whilst the winter maximum of 18.03 million square kilometres, recorded on 12 October (the equal-latest maximum date on record), was second behind 1986.

The mass balance change (the estimated change of the mass of ice from one year to the next) of the Greenland ice sheet in the year from September 2016 to August 2017 was well above the 1981–2010 average, due mainly to unusually heavy precipitation during autumn 2016. The mass balance change from September to December 2017 was close to average. Although the overall ice mass increased, this was only a small departure from the trend over the past two decades, with the Greenland ice sheet having lost approximately 3 600 billion tons of ice mass since 2002.

Mass balance change data for 2017 for glaciers outside major continental ice sheets are not yet available. For 2016, mass balance change, averaged across a set of 26 reference glaciers with data available at the time of writing, was approximately –900 mm water equivalent. This was a smaller decrease than in 2015, but close to the 2011–2016 mean. The glacial mass balance change has been negative in every year since 1988.

The northern hemisphere snow cover extent was near or slightly above the 1981–2010 average for most of the year, most significantly in May (9% above average, 12th highest on record). May snow cover extent was the highest since 1996, and the highest in Eurasia since 1985, with particularly strong anomalies in north-western Russia and northern Scandinavia, where May temperatures were well below average. Summer snow cover extent, which has been showing a strong downward trend, was close to the long-term average in 2017 for the first time in more than a decade, giving June, July and August the highest values since 2004, 2006 and 1998 respectively. Similar to most recent years, autumn snow cover extent was above average, although not to the same extent as in 2016, with October and November both ranking 9th highest. Snow cover extent returned to slightly below average in December. Contrasting precipitation anomalies during the 2016/2017 winter saw alpine snow cover well below average in most of the European Alps, but at or near record high levels in Corsica.

In the southern hemisphere, an extensive snow event in southern South America from 14 to 21 June saw continental snow cover extent reach 750 000 square kilometres, the highest since satellite monitoring began in 2005, whilst the alpine snowpack at high elevations in south-eastern Australia was the deepest since 2000.

MAJOR DRIVERS OF INTERANNUAL CLIMATE VARIABILITY IN 2017

There are several large-scale modes of variability in the world's climate that influence conditions over large parts of the world on seasonal to interannual timescales. The El Niño/Southern Oscillation (ENSO) is probably the best-known of the major drivers of interannual climate variability. The equatorial Indian Ocean is also subject to fluctuations in sea-surface temperatures, although on a less regular basis than the Pacific. The Indian Ocean Dipole (IOD) describes a mode of variability that affects the western and eastern parts of the ocean. The Arctic Oscillation (AO) and North Atlantic Oscillation (NAO) are two closely related modes of variability in the atmospheric circulation at middle and higher latitudes of the northern hemisphere. In positive mode, the subtropical high-pressure ridge is stronger than normal, as are areas of low pressure at higher latitudes, such as the "Icelandic" and "Aleutian" lows, resulting in enhanced westerly circulation through mid-latitudes. In negative mode, the reverse is true, with a weakened subtropical ridge, weakened higher-latitude low pressure areas and an anomalous easterly flow through mid-latitudes. The Southern Annular Mode (SAM), also known as the Antarctic Oscillation (AAO), is the southern hemisphere analogue of the AO.

In contrast with 2016, which saw the later part of one of the strongest El Niño events of the last 50 years, a neutral phase of ENSO prevailed for most of 2017. The year began with conditions slightly cooler than average in the central and eastern equatorial Pacific, consistent with the borderline cool neutral/weak La Niña conditions which had existed in the last part of 2016. These cool anomalies had weakened by February, before becoming re-established later in 2017. By November, conditions had cooled to the point where a weak La Niña event had been declared by most agencies.

Whilst there was no basin-wide El Niño in 2017, there was a sharp warming near the South American coast early in the year, of a type more often seen during El Niño events. Temperatures near the coast of Ecuador and Peru were more than 2 °C above average in February and March, before declining in the following months. These warm coastal temperatures were associated with significant flooding, particularly in Peru (something which had been largely absent during the previous year's El Niño), whilst there were also heavy rains and flooding in California to an extent which far exceeded that of the 2015/2016 El Niño.

The Indian Ocean Dipole was generally on the positive side of neutral for most of 2017, although the strength of the signal varied considerably between different datasets (the strongest cool signal in the eastern Indian Ocean was also south of the 10°S southern boundary of the area used to define IOD indices). The IOD state was associated with dry conditions in much of Australia between May and September, and with a return to average to above-average rains in the Horn of Africa late in the year after an extended period of drought.

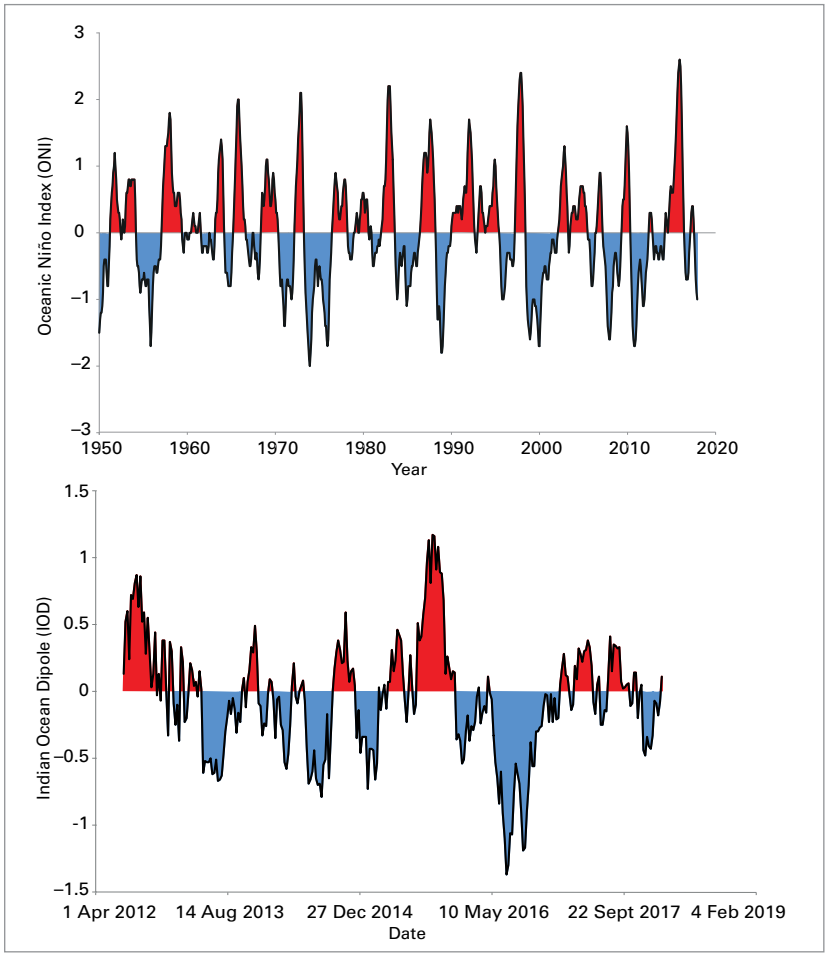

Figure 11. The Oceanic Niño Index (ONI) (top) and Indian Ocean Dipole (IOD) index (bottom). *(Source: prepared by WMO using data from the US National Oceanic and Atmospheric Administration (NOAA) Climate Prediction Center (ONI) and the Australian Bureau of Meteorology (IOD))*

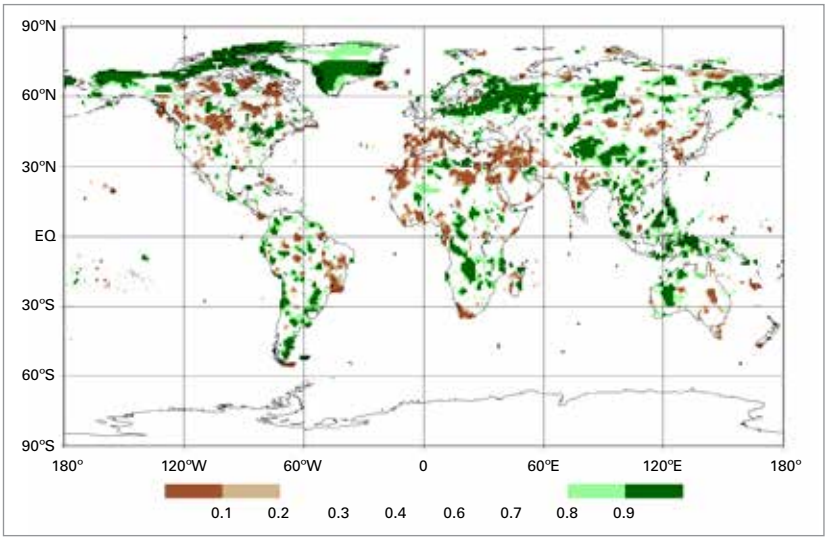

Figure 12. Annual total precipitation expressed as a percentile of the 1951–2010 reference period for areas that would have been in the driest 20% (brown) and wettest 20% (green) of years during the reference period, with darker shades of brown and green indicating the driest and wettest 10%, respectively *(Source: Global Precipitation Climatology Centre, Deutscher Wetterdienst, Germany)*

The Arctic Oscillation and North Atlantic Oscillation were both generally positive in their season of peak influence, January to March, with index values of +0.88 and +0.74 respectively, although in both cases these values were less strongly positive than in the equivalent period of 2016. These positive index values were associated with generally above-average temperatures in the 2016/2017 winter in most of Europe (despite a cold January) and eastern North America, and with dry winter conditions in the Mediterranean. Arctic Oscillation index values at the start of the 2017/2018 winter were near zero.

The Southern Annular Mode had its first period of sustained negative values for over two years in late 2016 and early 2017, with the three-month SAM index for November 2016 to January 2017 reaching –1.07, the strongest negative value since late 2013. Positive values then resumed for most of the remainder of 2017, although they were not as strong as those that prevailed for most of 2015 and 2016.

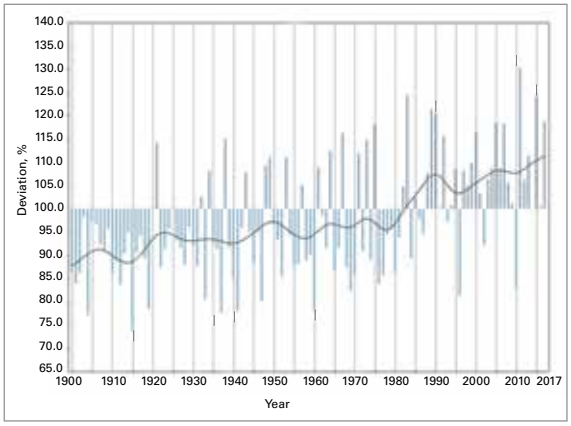

Figure 13. Annual precipitation for Norway in percentage of normal *(Source: Norwegian Meteorological Institute (Met.no))*

PRECIPITATION IN 2017

There were fewer areas with large precipitation anomalies in 2017 than there had been in 2015 or 2016, as the influence of the strong El Niño event of 2015/2016 ended.

The most extensive area with annual rainfall above the 90th percentile in 2017 was in north-east Europe, extending from northern European Russia as far west as northern Germany and southern Norway. European Russia had its second-wettest year on record (as did Russia as a whole) and Norway its sixth-wettest. Autumn was especially wet in the Baltic region, with Estonia and Lithuania both having their wettest autumn on record and Latvia its second-wettest.

Thailand had its wettest year on record, with national rainfall 27% above average. The south was especially wet with the east coast region 56% above average. However, the high rainfall was more evenly distributed through the year than it was in the previous record wet year of 2011. Even though that year's extreme flooding was not repeated, there were significant local floods from time to time, particularly in the south of the country early in the year. Rainfall above the 90th percentile also occurred in the Philippines, parts of eastern Indonesia and the interior of Western Australia.

Other areas with annual rainfall above the 90th percentile included parts of inland southern Africa, scattered areas in the southern half of South America east of the Andes, and around the Great Lakes in North America. Michigan had its wettest year on record, with very wet conditions also in the Great Lakes and St Lawrence region of Canada. Rainfall significantly above average also affected many parts of Central America and the Caribbean islands, with the largest anomalies in those parts of the Eastern Caribbean that were most affected by hurricanes.

Dry conditions with rainfall below the 10th percentile were most widespread around the Mediterranean, extending east as far as the Islamic Republic of Iran. They were especially

prominent in southern Europe, from Italy westwards to Portugal, in north-western Africa and in south-west Asia, from eastern Turkey and the western Islamic Republic of Iran south to Israel. A small but significant area with rainfall below the 10th percentile affected the far south-west of South Africa. Other major areas with rainfall below the 10th percentile in 2017 included parts of central India and eastern Brazil, and the North American Prairies on both sides of the United States-Canada border.

Monsoon season rainfall was generally fairly close to average in the Indian subcontinent (where all-India rainfall for June to September was 5% below average), although with local variations, including significantly above-average totals in much of Bangladesh and parts of far eastern India. Monsoon season rainfall was also fairly close to average in the Sahel of west and central Africa, although flooding in late August from local heavy rains caused significant losses in Niger. Rainfall in 2017 was also close to average over most of the more heavily populated parts of western and central Indonesia, in Singapore, in most of Japan (where an exceptionally wet October offset a dry first half of the year) and in north-western South America.

EXTREME EVENTS

Extreme events have many significant impacts in terms of casualties, other health effects, economic losses and population displacement.[15] They are also a major driver of interannual variability in agricultural production.

A DESTRUCTIVE NORTH ATLANTIC HURRICANE SEASON, BUT NEAR AVERAGE GLOBALLY

There were 84 tropical cyclones around the globe in 2017,[16] very close to the long-term average. A very active North Atlantic season was offset by near- or below-average seasons elsewhere. The North Atlantic had 17 named storms, and the seventh-highest value of Accumulated Cyclone Energy (ACE) on record, including a record monthly value for September. The Northeast and Northwest Pacific basins both had a near-average number of cyclones but relatively few severe cyclones, leading to below-average ACE values in both basins.

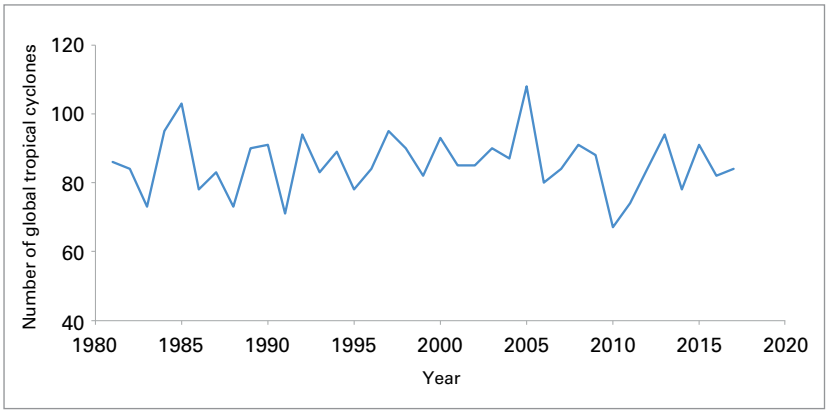

Figure 14. Total number of tropical cyclones globally, by year
(Source: WMO)

The 2016/2017 southern hemisphere season was below average on all measures, particularly in the first half of the season. Whilst the Australian region had a near-average number of cyclones, the south-west Indian Ocean and south-west Pacific (east of 160°E) were both well below average. The total hemispheric ACE was the lowest recorded since regular satellite coverage began in 1970.

Three exceptionally destructive hurricanes occurred in rapid succession in the North Atlantic in late August and September. *Harvey* made landfall in south Texas as a category 4 system, then remained near-stationary in the Houston area for several days, producing exceptionally prolonged extreme rainfall and severe flooding. An exceptional 1 539 mm of rain fell from 25 August to 1 September at a gauge near Nederland, Texas — the largest amount of rain ever recorded in a tropical cyclone in the United States — whilst the storm total rainfall was in the 900–1 200 mm range in much of metropolitan Houston.[17] One

[15] World Bank, 2017: A 360 degree look at Dominica post Hurricane *Maria*, 28 November, www.worldbank.org/en/news/feature/2017/11/28/a-360-degree-look-at-dominica-post-hurricane-maria

[16] Consistent with standard practice, the 2017 value quoted here is the sum of the values from January to December 2017 for northern hemisphere basins, and July 2016–June 2017 for southern hemisphere basins.

[17] National Hurricane Center, 2018: *National Hurricane Center Tropical Cyclone Report –Hurricane Harvey,* https://www.nhc.noaa.gov/data/tcr/AL092017_Harvey.pdf.

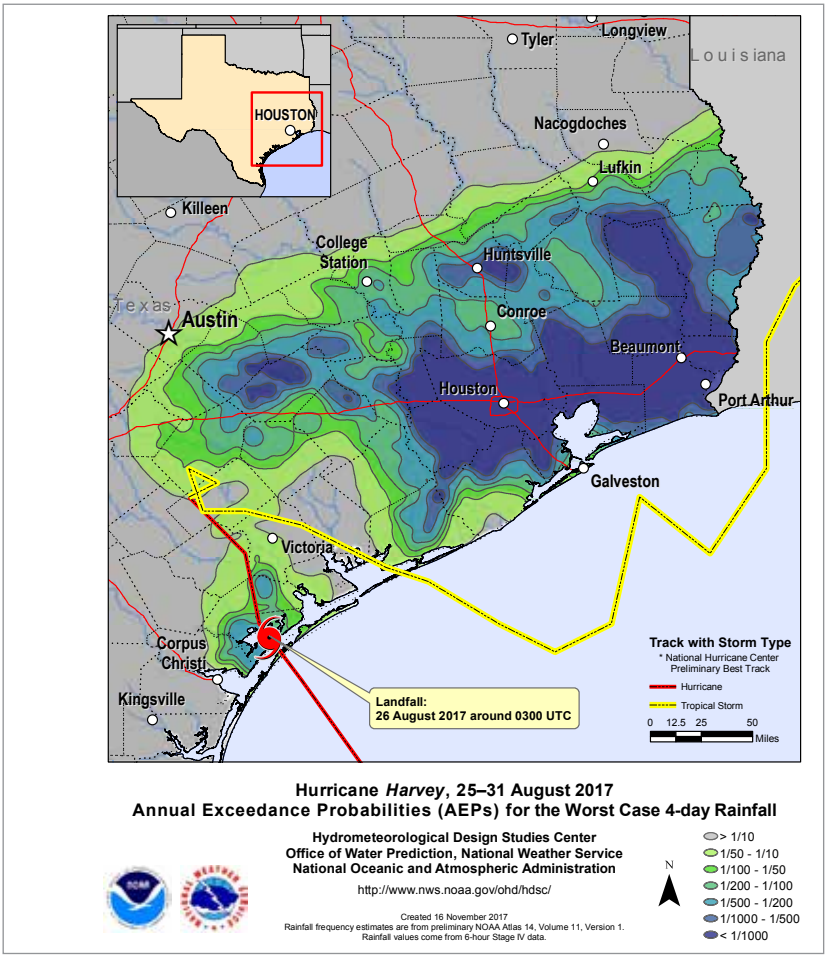

Figure 15. Annual exceedance probabilities for the peak 4-day rainfall during Hurricane *Harvey*, showing that much of the area from east Houston to the Texas-Louisiana border had 4-day rainfalls with an annual exceedance probability less than 1 in 1000. *(Source: US National Oceanic and Atmospheric Administration (NOAA)*

study[18] found that the maximum three-day rainfalls during Hurricane *Harvey* were made three times more likely by anthropogenic climate change.

Harvey was followed by Hurricane *Irma,* in early September, and by *Maria* in mid-September. Both hurricanes peaked at category 5 intensity, with *Irma* maintaining that intensity for 60 hours, which is longer than in any North Atlantic hurricane in the satellite era. *Irma*'s initial landfall, at near-peak intensity, led to extreme damage across numerous Caribbean islands, most significantly on Barbuda, which experienced near-total destruction, with only a few inhabitants having returned as of early 2018. Other islands to experience major damage included Saint Martin/Sint Maarten, Anguilla, St Kitts and Nevis, the Turks and Caicos Islands, the Virgin Islands and the southern Bahamas. *Irma* went on to track along the northern coast of Cuba, leading to extensive damage there, before making landfall in south-west Florida at category 4 intensity.

Hurricane *Maria* made initial landfall on Dominica at near-peak intensity, making it the first category 5 hurricane to strike the island, and leading to major destruction there. The World Bank estimates Dominica's total damages and losses from the hurricane at US$ 1.3 billion or 224% of its Gross Domestic Product (GDP). The storm weakened slightly but was still a category 4 hurricane when it reached Puerto Rico. *Maria* triggered widespread and severe damage on Puerto Rico from wind, flooding and landslides. Power was lost to the entire island, and had only been restored to just over half the population three months after the hurricane, whilst water supplies and communications were also severely affected.

All three of these hurricanes were assessed by the National Centers for Environmental Information (NCEI) as ranking in the top five for hurricane-related economic losses in the United States (alongside *Katrina* in 2005 and *Sandy* in 2012), with estimated costs of US$ 125 billion for *Harvey*, US$ 90 billion for *Maria* and US$ 50 billion for *Irma*.[19] *Irma* and *Maria* also led to substantial losses outside the United States. At least 251 deaths were attributed to the three hurricanes in the United States (including Puerto Rico and the US Virgin Islands) and 73 elsewhere.[20]

Other significant hurricanes during the 2017 North Atlantic season, both in October, were Hurricane *Nate*, which was associated with significant flooding in Central America

[18] Van Oldenborgh, G.J. et al., 2017: Attribution of extreme rainfall from Hurricane *Harvey*, August 2017. *Environmental Research Letters*, 12, 124009.

[19] The total losses reported by NCEI for these three hurricanes (central estimate US$265 billion) are higher than the assessment by Munich Re (US$215 billion, including losses outside the United States), but this difference is within the margin of uncertainty. It may also reflect differences in accounting for indirect economic losses.

[20] Unless otherwise stated, casualty and economic loss data reported in this statement are sourced from the EM-DAT database, Centre for Research on the Epidemiology of Disasters, Université catholique de Louvain, Belgium, www.emdat.be. For the 2017 North Atlantic hurricane season, casualties and economic losses for the United States and its territories were as reported by NCEI.

NORTH ATLANTIC HURRICANE SEASON 2017: INDUCED LOSS AND DAMAGE

When Hurricane *Irma* made landfall, it hit Barbuda with maximum sustained winds of 295 km/h, record rainfall and a storm surge of nearly three metres. Deaths were limited to one but an estimated 90% of properties were damaged. This prompted the Prime Minister to order the complete evacuation of all residents as Hurricane *Jose* approached. It was three weeks before residents were permitted to return, and three months later only an estimated 20% of the population had returned. The long-term impact remains to be seen, with damage and loss estimated at US$ 155 million, and recovery and reconstruction needs estimated at US$ 222.2 million[1] – together accounting for approximately 9% of the gross domestic product of Antigua and Barbuda.

Hurricane *Maria* proved still more devastating for Dominica. Total damages and losses were estimated at US$ 1.3 billion or 224% of GDP, with significant parts of the island's rainforest damaged and destroyed. This has implications for the whole of society: the losses incurred by the tourist sector alone are estimated at 19%, and 38% of housing was damaged.[2] *Maria* caused the longest blackout in the history of the United States in Puerto Rico, which affected 35% of the island's population for at least three months – continued problems following the hurricane may see the privatization of the Puerto Rico Electric Power Authority (PREPA), the largest publicly owned corporation in the United States.[3] The disaster prompted the Federal Emergency Management Agency to approve US$ 1.02 billion of assistance to the Individuals and Households Program and obligate US$ 555 million in Public Assistance grants.[4]

[1] Post-Disaster Needs Assessment (PDNA) carried out with the support of the European Union (EU), the United Nations Development Programme (UNDP), the World Bank and the Caribbean Disaster Emergency Management Agency (CDEMA).

[2] Government of the Commonwealth of Dominica, 2017: Post Disaster Needs Assessment – Hurricane *Maria*, September 18, 2017, https://reliefweb.int/sites/reliefweb.int/files/resources/dominica-pdna-maria.pdf

[3] Attributed to the Governor of Puerto Rico.

[4] Government of the United States of America, Department of Homeland Security, Federal Emergency Management Agency.

(especially Costa Rica and Nicaragua), and Hurricane *Ophelia*, which became the easternmost hurricane on record to reach major (category 3) intensity, before crossing Ireland as a transitioning extratropical storm and leading to widespread damage. *Ophelia*'s broader wind field also contributed to destructive wildfires in Portugal.

Whilst the number of severe cyclones in the Northwest Pacific in 2017 was low, a number of systems still brought widespread destruction and heavy casualties, mostly from flooding. The largest loss of life from a tropical cyclone in 2017 was in late December, when Typhoon *Tembin* (*Vinta*) crossed the island of Mindanao with a peak 10-minute wind speed of 36 m s^{-1} (70 kt), resulting in at least 129 deaths,[21] mostly from flooding. Two separate events in Vietnam, an unnamed tropical depression in October and Typhoon *Damrey* (*Ramil*) in early November, were both associated with over 100 deaths from flooding. The heaviest economic losses were from Typhoon *Hato* (*Isang*) in August, which hit Hong Kong, Macau and neighbouring areas of China on 23 August, with an estimated US$ 6 billion in losses and at least 32 deaths.[22] It was the strongest impact in Macau for more than 50 years.

The two most significant cyclones of the year in the North Indian Ocean were Cyclone *Mora* in late May, and Cyclone *Ockhi* in early December, both of which caused substantial casualties. The major impact of both cyclones was severe flooding and landslides associated with their respective precursor lows. Sri Lanka

[21] Philippines Office of Civil Defense, Situation Report 25, 7 February 2018.

[22] Reports from the China Meteorological Administration and the government of the Macao SAR.

Chris B. Pye

ST THOMAS, US VIRGIN ISLANDS
Hurricane *Irma* destruction

was badly affected by both cyclones, whilst *Ockhi* also had major impacts in southern India, including a great number of fishermen going missing at sea. The largest impacts from Northeast Pacific systems in 2017 were from flooding, with Tropical Storm *Lidia* leading to significant flooding in Mexico in August, and Tropical Storm *Selma* (the first recorded tropical cyclone to make landfall in El Salvador) doing likewise in El Salvador, Nicaragua and Honduras.

Although the number of tropical cyclones in the south-west Indian Ocean was below average, there were two which had major impacts. *Dineo*, with maximum 10-minute winds of 39 m s^{-1} (75 kt), was the first to make landfall in Mozambique since 2008 when it hit in early February. In addition to its effects in Mozambique, the subsequent overland low resulted in severe flooding in Zimbabwe and northern South Africa, and was the main contributor to the 246 flood-related deaths reported in Zimbabwe during the 2016/2017 rainy season.[23] *Enawo*, in early March, hit the east coast of Madagascar at near its peak intensity (10-minute winds of 57 m s^{-1} (110 kt)). *Enawo* had major impacts on Madagascar,[24] with at least 81 associated deaths reported and extensive damage to houses, infrastructure and crops. Agricultural losses were estimated by the World Bank at US$ 207 million, mostly from the destruction of vanilla plantations.

In the Southwest Pacific, Cyclone *Debbie* hit the east coast of Australia in late March, making landfall in the Whitsunday region with maximum 10-minute winds of 43 m s^{-1} (80 kt) after earlier peaking at 49 m s^{-1} (95 kt), leading to extensive wind and flood damage. The system then tracked south and south-east as a tropical low, with widespread major flooding, especially on the east coast near the Queensland-New South Wales border. The remnant system then went on to be largely responsible for major flooding in much of the North Island of New Zealand in early April. Insured losses for *Debbie* in Australia were approximately US$ 1.3 billion,[25] the second-highest on record for an Australian tropical cyclone. Cyclone *Donna* was the strongest May cyclone on record in the Southwest Pacific region, with peak 10-minute winds

[23] United Nations Office for the Coordination of Humanitarian Affairs (OCHA), 2017: Zimbabwe Flood Snapshot, https://reliefweb.int/sites/reliefweb.int/files/resources/zimbabwe_flood_snapshot_3march2017.pdf.

[24] World Bank, 2017: Estimation of Economic Losses from Tropical Cyclone Enawo, https://reliefweb.int/sites/reliefweb.int/files/resources/MG-Report-on-the-Estimation-of-Economic-Losses.pdf.

[25] Insurance Council of Australia, media release 6 November 2017.

reaching 57 m s^{-1} (111 kt) on 8 May, with some damage reported, especially in Vanuatu.

HIGH WINDS AND SEVERE LOCAL STORMS

There were a number of destructive severe thunderstorms in 2017, with central and eastern Europe particularly affected during the spring and early summer. Winds, exceeding 100 km/h during a thunderstorm resulted in widespread damage and at least 11 deaths in Moscow on 29 May. Other noteworthy storms included a severe hailstorm and tornado that affected the southern suburbs of Vienna on 10 July, a 165 km/h wind gust at Innsbruck on 30 July, a hailstorm with hailstones up to 9 cm in diameter in Istanbul on 27 July, and widespread thunderstorms that left 50 000 households without power in southern Finland on 12 August. Severe flash flooding affected parts of the Croatian coast on 11 September, with 283 mm of rain recorded in 12 hours at Zadar.

For the first time since 2011, the United States had an above-average tornado season, with a preliminary annual total of 1 406 tornadoes, 12% above the 1991–2010 average. However, the number of fatalities during the season (34) was below the long-term average. The most destructive storm of the season was a hailstorm that hit Denver on 8 May, with hailstones exceeding 5 cm in diameter. Insured losses from this event exceeded US$ 2.2 billion.

A severe windstorm (known locally as *Zeus*) affected France on 6–7 March. Peak gusts reached 193 km/h at Camaret-sur-Mer in Brittany, and the storm was rated by Météo-France as the most significant windstorm in France since 2010. Later in the year, a storm in late October produced wind gusts exceeding 170 km/h at high elevations and 140 km/h in the lowlands in Austria and Czechia, with 11 deaths reported in total.

FLOODING (NON-TROPICAL CYCLONE) AND ASSOCIATED PHENOMENA

One of the most significant weather-related disasters of 2017, in terms of casualties, was a landslide in Freetown, Sierra Leone, on 14 August, in which at least 500 deaths occurred.[26] Exceptionally heavy rain was a major contributor to this disaster; Freetown received 1 459.2 mm in the period from 1 to 14 August, about four times the average rainfall for this period. Another major landslide associated with heavy rainfall occurred in Mocoa, in southern Colombia, on 1 April, with at least 273 deaths reported.

Many parts of the Indian subcontinent were affected by flooding during the monsoon season between June and September, despite overall seasonal rainfall being near average over the region. The most serious flooding occurred in mid-August, after extremely heavy rainfall over a region centred on eastern Nepal, northern Bangladesh and adjacent areas of northern and north-eastern India. Mawsynram (India), near the Bangladesh border, received 1 479 mm in the four days from 9 to 12 August. Daily totals in excess of 400 mm also occurred near the India-Nepal border, and the Rangpur region of northern Bangladesh received 360 mm, approximately the average monthly total, on 11–12 August. Across the period as a whole, more than 1 200 deaths were reported in India, Bangladesh and Nepal,[27] whilst more than 40 million people were affected. The World Health Organization (WHO) noted that in Bangladesh alone more than 13 000 cases of waterborne diseases and respiratory infections were reported over three weeks in August,[28] whilst extensive damage was reported to public health facilities in Nepal.[29]

Earlier in the season, 292 deaths were reported in Sri Lanka in late May, principally in southern

---

[26] International Organization for Migration (IOM), 2017 : Sierra Leone Flood Response. Situation Report, 28 August 2017, https://reliefweb.int/sites/reliefweb.int/files/resources/SL%20Floods%20Sitrep%201.pdf.

[27] World Meteorological Organization, 2017: Rainfall extremes cause widespread socio-economic impacts, https://public.wmo.int/en/media/news/rainfall-extremes-cause-widespread-socio-economic-impacts.

[28] International Federation of Red Cross and Red Crescent Societies (IFRC), 2017: South Asia flood crisis: Disease outbreaks, funding shortages compound suffering of flood survivors, https://media.ifrc.org/ifrc/press-release/south-asia-flood-crisis-disease-outbreaks-funding-shortages-compound-suffering-flood-survivors/.

[29] World Health Organization (WHO), 2017: Nepal. Situation Report #5, https://reliefweb.int/sites/reliefweb.int/files/resources/who_sitrep-06sept2017.pdf.

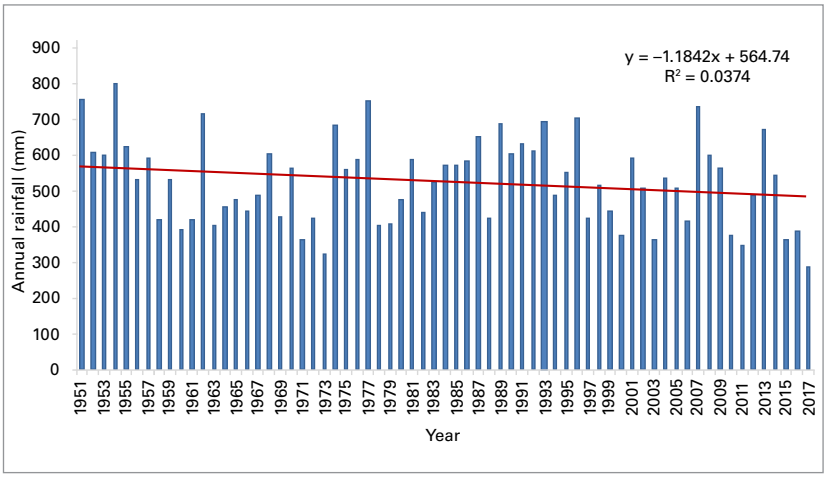

Figure 16. Annual rainfall for Cape Town, South Africa, 1951–2017. *(Source: South African Weather Service)*

and western parts of the country, due to heavy rains from the precursor low to Cyclone *Mora*. Ratnapura received 384 mm of rain in 24 hours on 25/26 May. Some 650 000 people were affected in some way by the floods, but the rains did little to alleviate significant drought in northern and eastern parts of Sri Lanka.[30] Cyclone *Mora* also had significant impacts in Bangladesh and Myanmar.[31] Heavy rains flooded thousands of hectares of crop and damaged poultry sheds, fishing nets and boats, severely eroding the livelihoods of communities that depend on agriculture and fisheries in the affected rural districts.

Flooding affected many parts of Peru in March, after sustained heavy rains. At least 75 deaths[32] were reported, and over 625 000 people were affected, including more than 70 000 who lost their homes. The Food and Agriculture Organization of the United Nations reported that there were significant crop production losses,[33] particularly maize, in the main producing regions of Lambayeque, Piura and Ica. Flooding of this type typically affects Peru during the late phase of El Niño events. Whilst there was no Pacific-wide El Niño during 2017, sea-surface temperatures near the Peruvian coast in March were 2 °C or more above average, values which would be more typical of an El Niño year than of a neutral year such as 2017. Major flooding occurred mid-year in parts of southern China, especially within the Yangtze River basin. The heaviest rain fell in the provinces of Hunan, Jiangxi, Guizhou and Guangxi. Peak totals during the period from 29 June to 2 July were in excess of 250 mm. Fifty-six deaths were reported and economic losses were estimated at more than US$ 5 billion.[34]

DROUGHT

The drought that affected significant parts of east Africa during 2016 continued into 2017. In the March to May rainy season, seasonal rainfall was at least 20% below average over most of Somalia, Kenya and southern Ethiopia, and more than 50% below average over most of the northern half of Kenya and parts of Somalia. There was some easing of conditions late in the year, with near- to above-average rainfall over most of the region in the October–December period. Reports for Somalia indicated that 6.7 million people were experiencing food insecurity as of October, this declined to 5.4 million by the end of December as crop and pasture conditions improved.[35]

Drought worsened significantly during 2017 in the Cape Province of South Africa. Following below-average rainfall in 2015 and 2016, Cape Town had its driest year on record in 2017 with a total of 285 mm (47% below the 1981–2010 average). The three-year period 2015–2017 was also the driest on record (36% below average). The dry conditions led to local water supplies becoming severely depleted, with no significant recovery as of early 2018. However, generally average to above-average rainfall further north in southern Africa during the 2016/2017 rainy season led to an improvement

[30] Food and Agriculture Organization of the United Nations (FAO) and World Food Programme (WFP), 2017: *Special Report. FAO/WFP Crop and Food Security Assessment Mission to Sri Lanka*, http://www.fao.org/3/a-i7450e.pdf.

[31] International Federation of Red Cross and Red Crescent Societies (IFRC), 2017: Emergency appeal revision. Bangladesh: Cyclone Mora, http://reliefweb.int/sites/reliefweb.int/files/resources/MDRBD019_RevEA.pdf.

[32] From information supplied by the United Nations Office for Disaster Risk Reduction (UNISDR).

[33] Food and Agriculture Organization of the United Nations (FAO), 2017: GIEWS – Global Information and Early Warning System. Country Brief: Peru, http://www.fao.org/giews/countrybrief/country.jsp?code=PER.

[34] From information supplied by the China Meteorological Administration.

[35] Food and Agriculture Organization of the United Nations (FAO), 2018: FSNAU-FEWS NET Technical Release, 29 January 2018, http://www.fsnau.org/in-focus/fsnau-fews-net-technical-release-january-29-2018.

in conditions there, with the total number of people experiencing food insecurity declining from 40 million at the peak of the 2014–2016 drought to 26 million in late 2017.[36]

Many parts of the Mediterranean region experienced significant drought in 2017, as did parts of central Europe. In the first part of 2017, the most severe anomalies were in Italy, which had its driest January to August on record (and went on to have its driest year, with annual rainfall 26% below the 1961–1990 average). Further north, Bratislava (Slovakia) had its driest December to August on record and southern Moravia (Czechia) its second-driest January to August. Later in the year the focus of the dry conditions was on south-west Europe. Spain had its driest autumn on record, the Provence-Haute Alpes-Côte d'Azur region in south-east France had its driest May to November, whilst Portugal had its driest April to December and its third-driest year (its four driest having all occurred since 2004). Autumn was also very dry in Morocco. The eastern Mediterranean was also badly affected by drought, including the eastern half of Turkey, Cyprus and most of Israel. The coastal plain of Israel had its driest year on record.

Drought also affected a region of central North America on both sides of the United States-Canada border. Particularly affected were the states of North Dakota and Montana, and the Prairie provinces of Canada, with areas of severe drought identified on both sides of the border.[37] After a period of prolonged drought, the 2016/2017 winter rainfall season brought heavy rains to much of California, and the Sierra Nevada snowpack was 66% above average, the heaviest since 1998. Large-scale evacuations were required in the state's north in February because of the risk of failure of the Oroville Dam. However, dry conditions resumed in the second half of the year, contributing to numerous major wildfires.

Although rainfall deficit was not particularly extreme during 2017, near-average to below-average rainfall resulted in a continuation of multi-year drought in many parts of Brazil north of 20°S, and in central Chile (where 2017 was the wettest year since 2008, but still drier than the long-term average). In the Asia-Pacific region, abnormally dry conditions were reported in the Korean Peninsula in the first half of 2017, whilst New Caledonia experienced significant drought, especially later in the year.

HEATWAVES, A REGULAR FEATURE OF 2017

There were numerous significant heatwaves around the world during 2017, in both the southern and northern hemisphere summers.

Southern South America experienced extreme heat on several occasions during the 2016/2017 summer. The heat peaked in late January, when numerous Chilean stations had their hottest days on record, including Santiago (37.4 °C) and Curico (37.3 °C) on the 25th, and Chillan (41.5 °C) and Concepcion (34.1 °C) on the 26th. The heat extended eastwards into Argentine Patagonia where Puerto Madryn reached 43.4 °C on 27 January, the highest temperature ever recorded so far south. It was also a notably hot summer in much of eastern Australia, where Moree had 54 consecutive days of 35 °C or above from 28 December 2016 to 19 February 2017, the longest such sequence on record in New South Wales. Numerous locations, including Moree (47.3 °C), Dubbo (46.1 °C), Scone (46.5 °C), Bathurst (41.5 °C) and Williamtown (45.5 °C) had their highest recorded temperature on 11–12 February.

Extreme heat affected south-west Asia at the end of May. The temperature at Turbat, in the far south-west of Pakistan, reached 54.0 °C on 28 May, a national record for Pakistan and (if confirmed)[38] an equal record for Asia. During this event, sites in the Islamic Republic of Iran, Oman and the United Arab Emirates also exceeded 50 °C.

[36] World Food Programme (WFP), 2018: Poor Rains and Crop Infestation Threaten Deeper Hunger Across Southern Africa. Media release, 9 February 2018.

[37] National Oceanic and Atmospheric Administration (NOAA), 2017: North American Drought Monitor, December 2017.

[38] This observation, and another of 54.0 °C at Mitribah (Kuwait), are currently being reviewed by a WMO evaluation committee.

SNOW IN THE ALGERIAN SAHARA (AIN SEFRA REGION)

NASA

There were numerous heatwaves during the European summer, particularly in the Mediterranean region. The most significant affected Turkey and Cyprus in late June and early July, the western Mediterranean (especially Spain and Morocco) in mid-July, and Italy and the Balkans in early August. All-time records were set in all three events, including Antalya, Turkey (45.4 °C on 1 July); Cordoba (46.9 °C on 13 July), Granada (45.7 °C on 12 July) and Badajoz (45.4 °C on 13 July) in Spain; and Pescara (41.0 °C on 4 August), Campobasso (38.4 °C on 5 August) and Trieste (38.0 °C on 5 August) in Italy.

The south-western United States had a very hot summer. Death Valley had the highest monthly mean temperature (41.9 °C) on record for an American station in July. Later in the season, record-high temperatures occurred in coastal California in early September, including San Francisco (41.1 °C on 1 September). Eastern China was another area to experience extreme summer heat, with records set at Shanghai (40.9 °C on 21 July) and at the Hong Kong Observatory (36.6 °C on 22 August, associated with offshore flow during Typhoon *Hato*).

SIGNIFICANT COLD PERIODS IN 2017

Whilst 2017 saw above-average annual mean temperatures over almost all inhabited land areas, there were still some noteworthy cold events during the year.

January was a cold month over much of central and south-east Europe. Several countries experienced their coldest January since 1987, with monthly mean temperatures more than 5 °C below average in places. The cold also extended to parts of northern Africa with snowfalls in some elevated parts of the Algerian Sahara.

A major late-season storm then affected the region on 20–21 April. Moldova was the hardest hit, with heavy falls of snow and freezing rain – exceptional for the time of year – causing extensive forest and agricultural damage. Following the storm, severe late-season frosts contributed to significant agricultural losses, estimated by Munich Re at EUR 3.3 billion,[39] across many countries, including Switzerland, Austria, Ukraine, Romania, and Slovenia. The losses were exacerbated in many areas by unusually early development of crops due to an unusually warm March.

Extreme cold affected parts of Argentina in July. Bariloche fell to –25.4 °C on 16 July, 4.3 °C below its previous record. Very low overnight temperatures also occurred in parts of south-eastern Australia in the first few days of July, with record lows set at locations including Sale, Deniliquin and West Wyalong.

[39] Munich Re, 2018: Spring frost losses and climate change – not a contradiction in terms, 29 January 2018, https://www.munichre.com/topics-online/en/2018/01/spring-frost?ref=social&ref=Facebook&tid=NatCat2017%20Review.

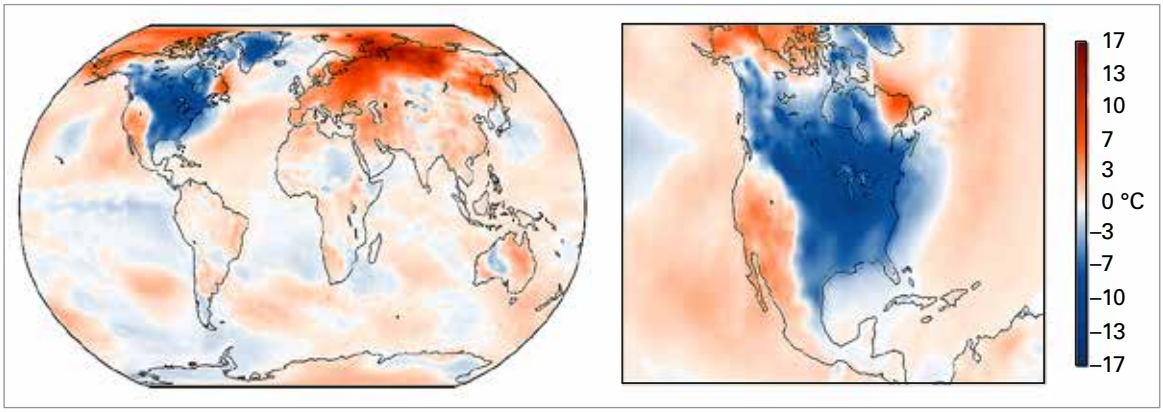

Figure 17. Temperature anomalies for the period 26 December 2017–5 January 2018 (relative to 1981–2010) showing the intense cold wave in eastern North America. *(Source: European Centre for Medium-range Weather Forecasts (ECMWF) Copernicus Climate Change Service)*

At the end of the year, a significant cold spell affected the north-eastern United States and eastern Canada, with temperatures remaining significantly below average for two weeks or more. The cold spell was more notable for its persistence than its intensity, with a number of locations setting or approaching records for the longest continuous period below certain thresholds: one example was Boston, which had a record seven consecutive days with maximum temperatures of 20 °F (–6.7 °C) or below from 27 December to 2 January.

GLOBAL ASSESSMENT OF TEMPERATURE EXTREMES

Whilst a fully global assessment of temperature extremes for 2017 is not yet possible, the GHCNDEX dataset[40] of extreme temperature indices can be used to assess values over those parts of the world for which there is coverage. For minimum temperatures, the main areas of coverage are Europe, North America, Australia and parts of Russia; for maximum temperatures, coverage also extends to much of Asia (except the south and south-west) and South Africa. There is little or no coverage in South or Central America, or in Africa outside South Africa.

Over the areas that do have coverage, maximum temperatures above the 90th percentile occurred on an average of 16.7% of days, the third-highest value on record after 2015 (18.5%) and 2016 (17.8%). They occurred locally on 25% or more of days in parts of southern Queensland (Australia) and the Iberian Peninsula, and on 20% or more of days in much of eastern Australia, central Asia and southern Europe. Only western Canada and parts of north-west Russia had values below 10%. Warm nights were not as prevalent as warm days, with the average global frequency (15.7%) below the average of the last 10 years.

Cold days, with maximum temperatures below the 10th percentile, occurred on 6.2% of days, the third-lowest value on record, whilst cold nights, with minimum temperatures below the 10th percentile, had the fifth-lowest value (5.7%). Cold extremes, both by day and night, were particularly uncommon in 2017 in north-western Europe, with values in a region stretching from the United Kingdom to Germany below 3% for cold days and 4% for cold nights. Values above 10% were found only in parts of Australia for cold nights, and in central Canada for cold days, although

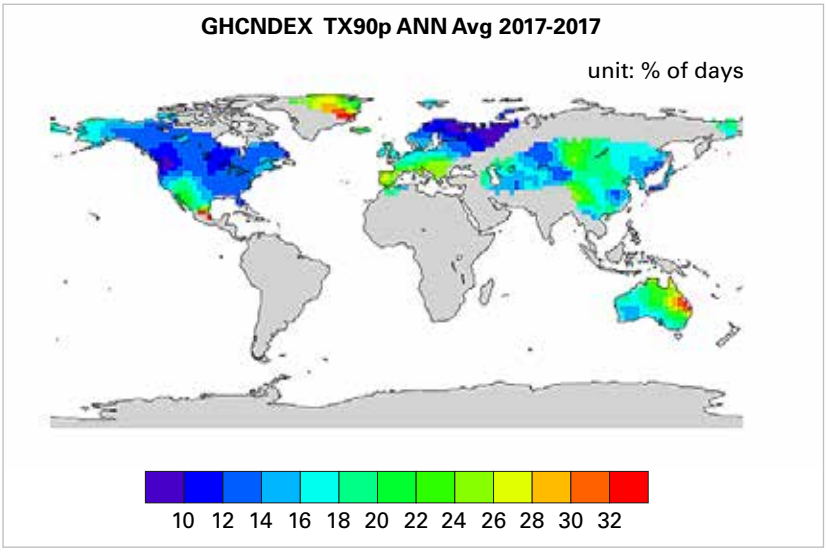

Figure 18. Percentage of days in 2017 with daily maximum temperatures above the 90th percentile, from the GHCNDEX dataset *(Source: University of New South Wales Climate Change Research Centre, Australia)*

[40] Donat, M.G. et al., 2013: Global Land-Based Datasets for Monitoring Climatic Extremes. *Bulletin of the American Meteorological Society*, 94:997–1006. This dataset uses a 1961–1990 baseline for the calculation of percentile thresholds.

much of the northern United States and southern Canada had a frequency of cold days between 8% and 10%.

HEAT AND DROUGHT CONTRIBUTE TO NUMEROUS DESTRUCTIVE WILDFIRES

Extreme heat and drought contributed to many destructive wildfires in various parts of the world in 2017. Whilst a return to near- or above-average rainfall contributed to reduced fire activity (compared with recent years) in various tropical regions, numerous mid-latitude regions had severe fire seasons.

Chile had the most significant forest fires in its history during the 2016/2017 summer, when exceptionally dry conditions during 2016 were followed by extreme heat in December and January. Eleven deaths were reported, and a total of 614 000 hectares of forest were burnt – the highest seasonal total on record and eight times the long-term average.[41] There were also significant fires during the 2016/2017 southern hemisphere summer in various parts of eastern Australia (especially eastern New South Wales) and in the Christchurch region of New Zealand, whilst the southern South African town of Knysna was badly affected by fire in June.

It was a very active fire season in the Mediterranean region. The worst single incident took place in central Portugal in June, where 64 people died in a fire near Pedrogao Grande. There were further major fire outbreaks in Portugal and north-western Spain in mid-October (exacerbated by strong winds associated with the circulation of Hurricane *Ophelia*), with a further 45 deaths reported. The area burned in Portugal in the period from January to October[42] was more than five times the 2007–2016 median. Other significant fires were reported, including in Croatia, France and Italy.

It was also an active fire season in western North America, both in the United States and Canada. A wet winter, which allowed the heavy growth of ground fuels, followed by a dry and hot summer, provided ideal conditions for high-intensity fires, the worst of which occurred north of San Francisco in early October. At least 44 people died, the worst loss of life in a wildfire in the United States since 1918. Insured losses from the fire were assessed as at least US$ 9.4 billion,[43] the worst for a wildfire anywhere in the world, even surpassing the 2016 Fort McMurray fires in Canada. Total economic losses for the 2017 California fire season were assessed at US$ 18 billion. A further fire north-west of Los Angeles in December became California's largest fire in modern history, and indirectly resulted in 21 deaths in flash floods and debris flows when heavy rains fell on the burnt area in early January.[44]

The total area burned in the contiguous United States in 2017 was 53% above the 2007–2016 average,[45] just short of the record set in 2015, whilst the area burned in the western provinces of Canada was also far above average, with over 1.2 million hectares burned in British Columbia, about eight times the 2006–2015 seasonal average.[46] Long-lived fires in British Columbia and the north-west United States also contributed to heavy smoke pollution across the region.

A significant tundra fire occurred in August in the Disko Bay area, on the central west coast of Greenland.

THE INFLUENCE OF ANTHROPOGENIC CLIMATE CHANGE ON EXTREME EVENTS

Determining the extent, if any, to which anthropogenic climate change has influenced the occurrence of extreme events has been an active area of research in recent years.

---

[41] From information supplied by the Chilean Directorate of Meteorology.

[42] Portuguese Institute for Nature Conservation and Forests, http://www.icnf.pt/portal/florestas/dfci/Resource/doc/rel/2017/8-rel-prov-1jan-30set-2017.pdf.

[43] California Department of Insurance, media release of 6 December 2017, http://www.insurance.ca.gov/0400-news/0100-press-releases/2017/release135-17.cfm.

[44] National Centers for Environmental Information (NCEI), National Climate Reports for December 2017 and January 2018.

[45] National Interagency Coordination Center, Wildland Fire Summary and Statistics – Annual Report 2017 https://www.predictiveservices.nifc.gov/intelligence/2017_statssumm/intro_summary17.pdf.

[46] British Columbia Wildfire Service, http://bcfireinfo.for.gov.bc.ca/hprScripts/WildfireNews/Statistics.asp.

CALIFORNIA, UNITED STATES
October wildfires

NASA

Such analyses are now routinely published in the peer-reviewed literature, many of them as part of an annual report prepared as a supplement to the *Bulletin of the American Meteorological Society* (BAMS).

The most-recently published BAMS report included 27 analyses of extreme events that occurred in 2016 (some of them multiple analyses of the same event), and found that anthropogenic climate change was a significant driver of the frequency of the event concerned in 21 of the 27 cases. In particular, of 15 analyses that assessed extreme temperature events (either on land or in the ocean), 13 found that their probability had been significantly influenced by anthropogenic climate change in the "expected" direction (that is, that a warm event had become more likely or a cold event less likely). One counter-example of interest was a frost event in south-western Australia in September 2016, where it was found that anthropogenic climate change had significantly increased the chance of the circulation anomalies which were the primary driver for the event (notwithstanding the background warming signal). As in previous years, anthropogenic signals were found less consistently for extreme precipitation events, with such signals being found (in three different analyses) for extremely high rainfall in eastern China during the summer of 2016, but not for extreme precipitation events in other parts of the world.

Given the timeframes involved, few studies of 2017 events have yet been published in the peer-reviewed literature. One exception is an assessment of the extremely high rainfall associated with Hurricane *Harvey*. The WMO Expert Team on Climate Impacts on Tropical Cyclones also found[47] that, whilst there is no clear evidence that climate change is making the occurrence of slow-moving, land-falling hurricanes more or less likely, it is probable that anthropogenic climate change made rainfall rates more intense, and that ongoing sea-level rise exacerbated storm surge impacts. Assessments of recent events – most of which use methods that have been documented in the peer-reviewed literature, although the assessments themselves are not – are regularly published shortly after the event through a variety of channels, and it is likely that many of these events will be documented in the peer-reviewed literature in due course.

[47] WMO expert team statement on Hurricane *Harvey*, https://public.wmo.int/en/media/news/wmo-expert-team-statement-hurricane-harvey.

ATTRIBUTION OF EXTREME CLIMATE EVENTS

A common question when an extreme climate event happens is "was this event caused by climate change?". Scientists address this question in a different way: "Was the chance of this event happening affected by human influences on the climate, and if it was, by how much?".

Answering this question has become a very active area of research in the last few years. Whilst a range of approaches has been used, the most common is to use climate models. The approach consists in running these models with all known climate forcings, both anthropogenic and natural, and with natural forcings only. Comparing the probability of the event in question using the two sets of model runs allows the attribution of the event to anthropogenic versus natural factors. This is often expressed as the Fraction of Attributable Risk (FAR), which is the probability that the event was the result of anthropogenic influence on climate as opposed to natural variability.

Many of these studies have found that the probability of the extreme event has been influenced by human activity, either directly, or indirectly through, for example, affecting the likelihood of occurrence of an unusual circulation anomaly which triggered the extreme event; sometimes in conjunction with other influences such as the El Niño/Southern Oscillation (ENSO). Of a set of 131 studies published between 2011 and 2016 in the *Bulletin of the American Meteorological Society*, 65% found that the event's probability was significantly affected by anthropogenic activities.

The strongest anthropogenic influence has been found on temperature extremes: the likelihood of warm extremes increases and that of cold extremes decreases. This is especially true for events considered over large areas and over a long period of time, such as a season or a year. As an example, it was found that the 2016 record-breaking global mean temperature would have been almost impossible without human activity.[1] Because there is a higher level of "natural" variability at individual locations and over shorter timescales, it is more difficult to find a significant human signal in the occurrence of short-term extremes at specific places, although studies of that type are also starting to emerge.

It has been more difficult to identify anthropogenic influence in the attribution of precipitation extremes. Whilst some studies have found that the probability of some extreme precipitation events was increased, most often indirectly, by climate change, for many other studies the results have been inconclusive. This is because the underlying long-term climate signal in extreme precipitation is less clear than it is for temperature and, because extreme precipitation events typically occur on shorter spatial scales than extreme temperature events.

At present, attribution studies are mostly carried out in research mode and the most common platform for publishing these studies is through the traditional peer-reviewed literature. This is mostly done through an annual supplement to the State of the Climate report published in the *Bulletin of the American Meteorological Society*. Such studies usually appear several months following the occurrence of the event under consideration.

For some types of extremes, especially extremes defined using standard indices, such as national mean monthly temperature, methods have been developed which allow an assessment of the FAR for the event in close to real time. At present, most such reports are published through other channels than the National Meteorological and Hydrological Services (NMHSs) such as blogs, university or NGO websites, or the media. Operational attribution services under the auspices of NMHSs or Regional Climate Centres are in their infancy, although many individual NMHS scientists have contributed to the studies that are currently being published. Nevertheless, it is expected that there will be substantial progress in this area in the next few years due to the increased demand from governments, the public and the media for these services on quasi-real time.

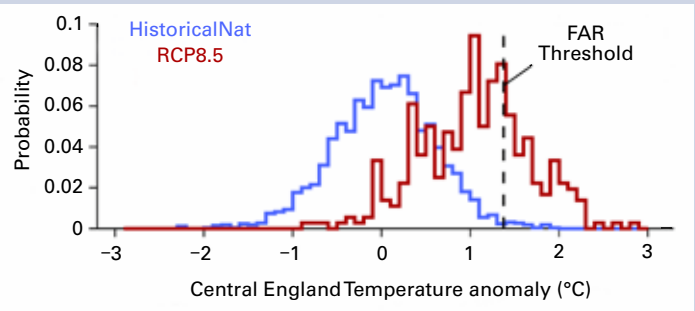

Probability distribution of annual mean Central England Temperature under natural (blue) and RCP 8.5 (brown) model simulations as of 2006, with the 2006 value (the highest on record) shown as a black dashed line (*Source: Andrew King, University of Melbourne, Australia)*

[1] Knutson, T.R. et al., 2017 : CMIP5 model-based assessment of anthropogenic influence on record global warmth during 2016. *Bulletin of the American Meteorological Society*, 99:S11-S15.

Climate risks and related impacts

Climate-related extreme events and disasters take a heavy toll on human well-being and on various sectors of national economies. The year 2017 was particularly severe for disasters with high economic impacts. Munich Re assessed total disaster losses from weather and climate-related events in 2017 at US$ 320 billion,[48] the largest annual total on record (after adjustment for inflation).

AGRICULTURE AND FOOD SECURITY

Exposure and vulnerability to extreme events can destroy agricultural assets and infrastructure, causing serious damage to the livelihoods and food security of millions of people. A concern for the World Food Programme (WFP) is that more than 80% of the world's food-insecure people live in countries with degraded environments prone to natural hazards. When climate-related events occur, the situation of already-vulnerable people can quickly deteriorate into food and nutrition crises. Problems of acute food insecurity and malnutrition tend to be magnified where natural hazards such as droughts and floods compound the consequences of conflicts.[49]

The disruption of agricultural production in rural areas of developing countries affects the already fragile livelihoods of the poorest and most vulnerable people in particular. A review carried out by FAO found that agriculture (crops, livestock, fisheries, aquaculture and forestry) accounted for 26% of all the damage and loss associated with medium to large-scale climate-related disasters. [50]

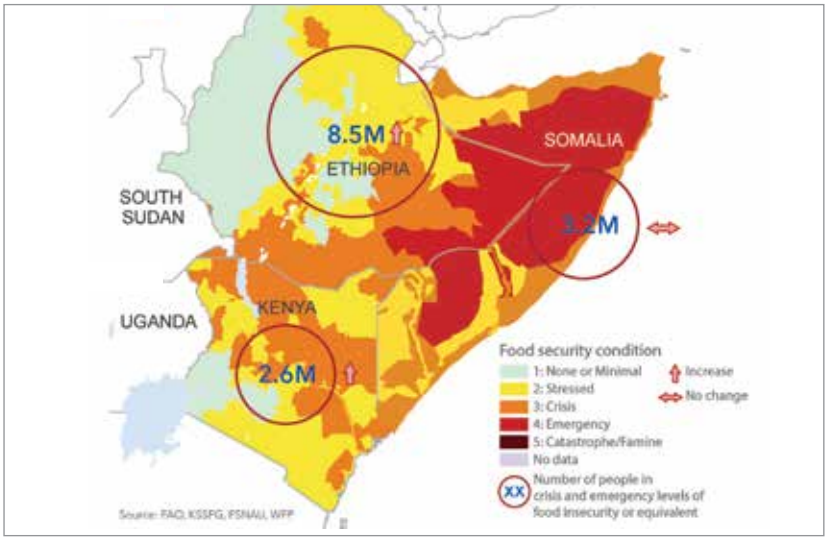

Figure 19. Number of severely food-insecure people in Kenya, Somalia and Ethiopia (*Source: Horn of Africa: Humanitarian Impacts of Drought – Issue 9, 20 August 2017 (OCHA)*)

In the Horn of Africa, rainfall deficits led to the failure of the 2016 rainy season, followed by a harsh January–February 2017 dry season, and a poor March–May rainy season. As a result, the number of food-insecure people rose significantly in Eastern Africa.[51] The most affected areas include southern and south-eastern Ethiopia, northern and coastal Kenya, almost all of Somalia, south-eastern areas of South Sudan and north-eastern areas of Uganda. In Somalia, as of June 2017, more than half of the cropland was affected by drought, and herds had reduced by 40 to 60% since December 2016 due to increased mortality and distress sales.

In Ethiopia, prolonged drought jeopardized crop production and caused a reduction in the availability of pasture, severely constraining the purchasing power of pastoral households. In drought-affected areas of Kenya, according to the Vegetation Condition Index (VCI), as of May 2017 drought was associated with a sharp increase in staple crop prices coupled with declining livestock prices and consequent erosion of livelihoods and threat to food security.[52]

---

[48] Munich Re, 2018: Hurricanes cause record losses in 2017 – The year in figures. Release of 4 January 2018. The losses quoted by Munich Re include both insured and non-insured losses, but may calculate indirect economic losses (e.g. business interruption) in a different way than some other sources.

[49] Food and Agriculture Organization of the United Nations (FAO), International Fund for Agricultural Development (IFAD), United Nations Children's Fund (UNICEF), World Food Programme (WFP) and World Health Organization (WHO), 2017: *The State of Food Security and Nutrition in the World 2017 – Building resilience for peace and food security.* FAO, Rome, http://www.fao.org/3/a-I7695e.pdf.

[50] Food and Agriculture Organization of the United Nations (FAO), 2017:*The Impact of Disasters on Agriculture – Assessing the information gap*, http://www.fao.org/3/a-i7279e.pdf.

[51] United Nations Office for the Coordination of Humanitarian Affairs (OCHA), 2017: Horn of Africa: Humanitarian Impacts of Drought, 9 (10 August 2017), https://reliefweb.int/report/somalia/horn-africa-humanitarian-impacts-drought-issue-9-10-aug-2017.

[52] Food and Agriculture Organization of the United Nations (FAO), 2017: Global Information and Early Warning System on Food and Agriculture (GIEWS). Special Alert No. 339. Region: East Africa, http://www.fao.org/3/a-i7537e.pdf.

DATA FOR MONITORING IMPACTS OF CLIMATE-RELATED EXTREME EVENTS AND DISASTERS

At the Seventy-first Session of the United Nations General Assembly[1] and the Forty-eighth Session of the United Nations Statistical Commission,[2] the data and indicators for the measurement of progress in achieving the global targets of the Sendai Framework for Disaster Risk Reduction 2015–2030 and of the 2030 Agenda for Sustainable Development were adopted. This enabled integrated monitoring and reporting by countries of progress in managing disaster and climate risk and the corollary impacts, using multi-purpose datasets and common indicators.

Data are currently available in most countries to allow some degree of measurement of the impact of climate-related extreme events and disasters – including via the growing number of national disaster loss accounting systems – as detailed in the Sendai Framework Data Readiness Review 2017.[3] However, considerable work is required if countries are to be able to monitor the agreed indicators in the manner anticipated by the two intergovernmental working groups – the Open-ended Intergovernmental Expert Working Group on Indicators and Terminology Relating to Disaster Risk Reduction (OIEWG) and the Inter-agency and Expert Group on Sustainable Development Goal Indicators (IAEG-SDGs). Many countries are confronted with challenges related to data availability, accessibility and quality, which will need to be addressed if data are to be sufficiently consistent and comparable to allow meaningful measurement of progress and impact.

Work is ongoing with the international statistical community to address some of these challenges. The outcomes of the Expert Group on Disaster-related Statistics will be presented at the Seventy-fourth Session of the Economic and Social Commission for Asia and the Pacific. They include the development of the disaster-related statistical framework (DRSF) to monitor the achievement of the global targets of the Sendai Framework and the Sustainable Development Goals.

Established by the Conference of European Statisticians of the United Nations Economic Commission for Europe, the Task Force on Measuring Extreme Events and Disasters is clarifying the role of official statistics in providing data related to extreme events and disasters, as well as possible support of national statistical offices to the implementation of the Sendai Framework and the 2030 Agenda.

Countries are supported in systematic data entry and reporting by the Sendai Framework Monitoring system, an online monitoring facility which became available on 1 March 2018, and which is supported by detailed guidance on metadata and computational methodologies. The integration of monitoring and reporting with The Paris Agreement will be discussed at the Thirteenth Meeting of the United Nations Framework Convention on Climate Change (UNFCCC) Adaptation Committee.

---

[1] Resolution (A/RES/71/276) approving the Report of the Open-ended Intergovernmental Expert Working Group on Indicators and Terminology relating to Disaster Risk Reduction (A/71/644).

[2] Report of the Inter-agency and Expert Group on Sustainable Development Goal Indicators – Note by the Secretary-General (E/CN.3/2017/2).

[3] United Nations Office for Disaster Risk Reduction (UNISDR): Sendai Framework data readiness review 2017 – Global summary report, https://www.preventionweb.net/publications/view/53080.

In the Philippines, over the last two decades, 15 times more infants have died in the 24 months after typhoons than in the typhoons themselves. Of those infants, 80% were girls.[53] In Ethiopia, children born in an area affected by disasters are 35.5% more likely to be malnourished and 41% more likely to be stunted.[54]

Over the last three years, agricultural production and related livelihoods were heavily compromised by recurrent and intense floods in many countries. In Malawi, the 2015 floods resulted in more than US$ 60 million in damage and losses to crops, livestock, fisheries and forestry assets, and production flows. More than 37% of the total economic impact of the 2015 floods in Myanmar occurred in the agricultural sector.[55]

In 2017, several flood events affected the agricultural sector, especially in Asian countries. Heavy rains in May 2017 triggered severe flooding and landslides in south-western areas of Sri Lanka. The adverse impact of floods on crop production further aggravated the food security conditions in the country already stricken by drought.[56] In July 2017, localized floods in south and central Myanmar contributed to losses in paddy crop, stored food and livestock, and affected at least 200 000 people in the Magway, Sagaing, Bago and Ayeyarwady regions and Mon State. It was the third consecutive year in which severe floods affected Myanmar during the monsoon season.

Population affected (in millions) due to floods in Bangladesh, India and Nepal, as of 24 August 2017

Country	*Total number of people affected*
Bangladesh	6.9
India	32.1
Nepal	1.7

Source: United Nations Office for the Coordination of Humanitarian Affairs (OCHA)

Excess precipitation in late March and early April 2017 triggered floods in north-eastern agricultural areas of Bangladesh, affecting crop production in the Sylhet, Dhaka and Mymensingh divisions in particular.[57] The monsoon season in South Asia brought the worst flooding in the region for years. Between June and August 2017, flooding in Nepal, Bangladesh and northern India affected millions of people and caused death and displacement across the three countries.

The end of the climate anomalies associated with the 2015/2016 El Niño, both on land and in the ocean, resulted in improved agricultural and fisheries production in some areas.[58] More normal rainfall patterns have contributed to two successive record-breaking global cereal harvests since 2015. World wheat production hit an all-time high in 2016 and is expected to remain at near-record levels in 2017, mainly due to larger crops in India and the Russian Federation. More abundant rains since mid-2016 in India, Thailand and the Philippines have increased rice output to a level that marked recoveries in these countries. As a result, world rice production reached a fresh peak in 2016 and was expected to expand further in the 2017 season. As to annual oilcrops, global production recovered swiftly in 2016/2017, actually posting a new record, and is anticipated to grow modestly

[53] Anttila-Hughes, J. and S. Hsiang, 2013: Destruction, Disinvestment, and Death: Economic and Human Losses Following Environmental Disaster. Available at SSRN: http://ssrn.com/abstract=2220501.

[54] Intergovernmental Panel on Climate Change (IPCC), 2007: Fourth Assessment Report, https://www.ipcc.ch/report/ar4/.

[55] Government of Myanmar. (2015). Myanmar. Post-disaster needs assessment of floods and landslides, July–September 2015, http://documents.worldbank.org/curated/en/646661467990966084/Myanmar-Post-disaster-needs-assessment-of-floods-and-landslides-July-September-2015.

[56] Food and Agriculture Organization of the United nations (FAO) and World Food Programme (WFP), 2017: *Special Report. FAO/WFP Crop and Food Security Assessment Mission to Sri Lanka*, http://www.fao.org/3/a-i7450e.pdf.

[57] Food and Agriculture Organization of the United nations (FAO), 2017: GIEWS – Global Information and Early Warning System. Country Brief: Bangladesh, http://www.fao.org/giews/countrybrief/country.jsp?code=BGD.

[58] Food and Agriculture Organization of the United Nations (FAO), 2017: *Food Outlook – Biannual Report on Global Food Markets*, November 2017, http://www.fao.org/3/a-I8080e.pdf.

in 2017/2018. Conversely, the recovery in palm oil production was more gradual and is expected to revert to its usual growth rate only in 2018. There was also a strong recovery in the Anchoveta fishery off the Pacific coast of South America as sea-surface temperatures in the region reverted to near average.

HEALTH

The global health impacts of heatwaves depend not only on the overall warming trend, but also on how heatwaves are distributed across the area where people live. Recent research shows that the overall risk of heat-related illness or death has climbed steadily since 1980, with around 30% of the world's population now living in climatic conditions that deliver potentially deadly temperatures at least 20 days a year.[59] Between 2000 and 2016, the number of vulnerable people exposed to heatwave events has increased by approximately 125 million.[60]

In cholera-endemic countries, an estimated 1.3 billion people are at risk, while in Africa alone about 40 million people live in cholera "hotspots".[61] These cholera "hotspots" have been identified across most endemic countries facing recurrent and predictable cholera outbreaks, often coinciding with the rainy season. The World Health Organization has recognized that large cholera outbreaks in eastern and central, and later southern Africa were likely aided by El Niño-driven weather conditions that accelerated transmission across the region starting in mid-2015, with control efforts still underway in several countries in 2017. Flood events are also often associated with outbreaks of water-borne diseases or those linked to poor sanitation, as was reported in Bangladesh during the August 2017 floods.

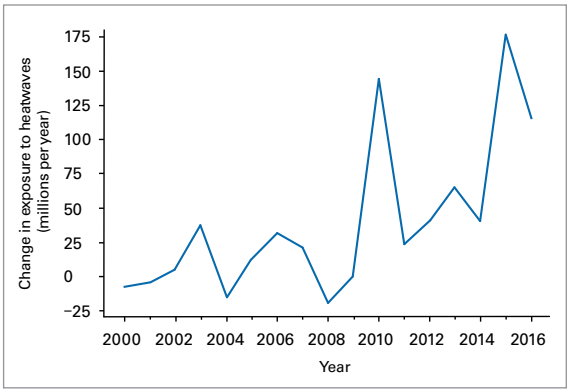

Figure 20. The change in exposure (in people aged over 65 years) to heatwaves from 2000 to 2016 relative to the heatwave exposure average from 1986 to 2008
(Source: World Health Organization (WHO))

POPULATION DISPLACEMENT

One of the adverse consequences of climate variability and change is population displacement. Most such displacement is internal and linked to sudden onset of extreme weather events. However, slow onset phenomena, such as droughts, desertification, coastal erosion and sea-level rise, can also lead to internal and cross-border displacement. These slow-onset events can act as a threat multiplier by, for example, exacerbating conflict which, in turn, can contribute to population displacement.

In 2016, weather-related disasters displaced 23.5 million people.[62] As in previous years, the majority of those internal displacements were associated with floods or storms and occurred in the Asia-Pacific region. The most striking example of displacement due to major climate events is from Somalia, where it was reported that 892 000 people were displaced internally, mostly in the first half of 2017.[63] Of the displaced people who were surveyed, approximately 90% indicated that drought was the primary reason for displacement, while the remaining 10% gave reasons closely related to drought or cited drought as a contributing factor, such as food or livelihood insecurity.[64]

[59] Mora C. et al., 2017: Global risk of deadly heat. *Nature Climate Change*, 7. DOI:10.1038/nclimate3322.

[60] Watts N. et al., 2017: The Lancet Countdown on Health and climate change: From 25 years of inaction to a global transformation for public health. *Lancet*, 30 October 2017.

[61] World Health Organization (WHO), 2017: Weekly epidemiological record, No. 22, 2 June 2017, http://apps.who.int/iris/bitstream/10665/255611/1/WER9222.pdf?ua=1.

[62] Internal Displacement Monitoring Centre (IDMC), 2017: Global Report on Internal Displacement 2017, http://www.internal-displacement.org/global-report/grid2017/pdfs/2017-GRID.pdf.

[63] Office of the United Nations High Commissioner for Refugees (UNHCR), 2018: Somalia. UNHCR Emergency Response at 31 December 2017, https://reliefweb.int/report/somalia/somalia-unhcr-emergency-response-31-december-2017.

[64] As of 23 June, 687 906 Somali IDPs interviewed by the UNHCR-led Protection & Return Monitoring Network (PRMN) indicated that drought was the primary reason for displacement, while 72 688 IDPs indicated that drought was a contributing factor, https://data2.unhcr.org/en/documents/download/58290.

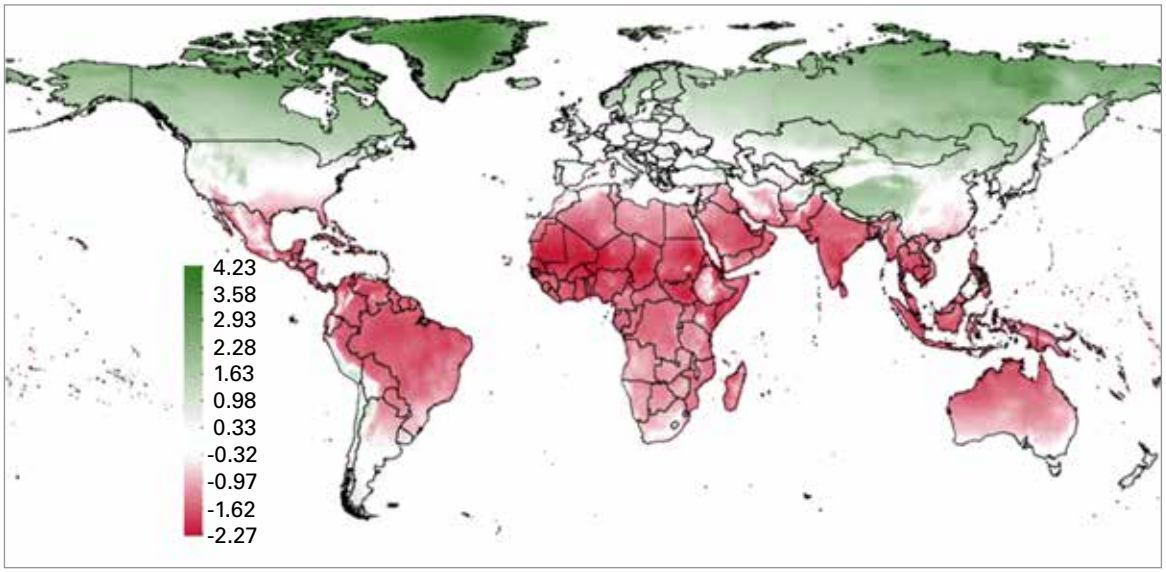

Figure 21. The effect of a 1 °C increase in temperature on real per capita output at the grid level.
(Sources: Natural Earth; ScapeToad; United Nations World Population Prospects: The 2015 Revision; World Bank Group Cartography Unit; and IMF staff calculations)

ECONOMIC IMPACTS

The International Monetary Fund (IMF) World Economic Outlook published in October 2017[65] indicates that increases in temperature have uneven macroeconomic effects. Adverse consequences are concentrated in regions with relatively hot climates, where a disproportionately large number of low-income countries are located. In these countries, a rise in temperature lowers per capita output, in both the short and medium term, by reducing agricultural output, suppressing the productivity of workers exposed to heat, slowing investment and damaging health.

The analysis confirms the existence of a statistically significant nonlinear effect of temperature on per capita economic growth. In countries with high average temperatures, an increase in temperature dampens economic activity, whereas it has the opposite effect in much colder climates.

For the median emerging market economy, a 1 °C increase from an average annual temperature of 22 °C lowers growth in the same year by 0.9%. For a median low-income developing country, with an annual average temperature of 25 °C, the effect of a 1 °C increase in temperature is even larger: growth falls by 1.2%. Countries whose economies are projected to be significantly adversely affected by an increase in temperature produced only about 20% of global GDP in 2016; however, they are currently home to nearly 60% of the global population and are projected to be home to more than 75% by the end of the century.

[65] International Monetary Fund, 2017: *World Economic Outlook, October 2017. Seeking Sustainable Growth: Short-Term Recovery, Long-Term Challenges*, https://www.imf.org/en/Publications/WEO/Issues/2017/09/19/world-economic-outlook-october-2017.

Vector-borne diseases: Zika in the Americas

Ángel G. Muñoz,[1] Rachel Lowe,[2] Anna M Stewart-Ibarra,[3] Joy Shumake-Guillemot,[4] Madeleine Thomson[1]

Vector-borne diseases are highly climate sensitive and favourable climate conditions can trigger and amplify disease transmission. Warm temperatures increase virus replication rates and drive the development of juvenile mosquitoes, adult feeding and egg laying behaviour. Rainfall excess and deficit have similar outcomes in terms of mosquito proliferation, as containers such as domestic pots, tires, drums and tanks tend to create suitable breeding sites in both cases.

The emergence of the Zika virus (ZIKV) epidemic, mainly carried by the *Aedes* mosquito in Latin America and the Caribbean in 2014–2016, occurred during a period of severe drought and unusually high temperatures developed since at least 2013 (see top and middle panels of the figure). These conditions have been shown to be associated with a cross-timescale combination of signals including the 2015/2016 El Niño event, decadal variability and climate change (Muñoz et al., 2016*a*,*b*).

A common approach to assess the potential risk of transmission of *Aedes*-borne epidemics is via the estimation of the basic reproduction number, R_0, which is in general a function of environmental variables, such as air temperature, and ento-epidemiological parameters (Mordecai et al, 2017). Using an R_0 model which considers the two most common *Aedes* mosquitoes in Latin America and the Caribbean, a recent study (Muñoz et al., 2017) showed that high temperatures enhanced the risk of transmission during the 2014–2016 ZIKV epidemic, and that neither El Niño nor climate change can be independently blamed for this event. While the potential risk of transmission signal (black curve in the bottom panel of the figure) is consistent with long-term temperature increase due to global warming and with inter-annual climate variability modes (filled red/blue curve shown in bottom panel of the figure) such as El Niño, other non-climatic factors come into play to explain the 2014–2016 ZIKV epidemic.

In fact, in addition to suitable climate conditions, the rapid transmission that occurred in the initial Brazilian outbreak appears to have been aided by a combination of factors including a massive susceptible population, alternative non-vector transmission, and a highly mobile population (Lowe et al., 2018). Furthermore, the occurrence of shocks such as natural disasters can also exacerbate population vulnerability. This was observed following the major earthquake in coastal Ecuador in April 2016, which seemingly enhanced the ZIKV transmission in that region where suitable hot and dry local climate conditions were already present (Sorensen et al., 2017).

Currently, local ZIKV transmission and the associated and resulting fetal malformations and neurological disorders continue to be monitored and recorded in the region and worldwide. Predictions of the timing and magnitude of outbreaks of multiple arboviruses, including ZIKV, can be improved using a combination of climate forecasts and sero-prevalence survey data (Lowe et al., 2017). For example, real-time seasonal climate forecasts have been used to produce dengue early warnings for Brazil (Lowe et al., 2014, 2016), and the use of the R_0 model mentioned above and state-of-the-art climate forecasts provided by the North American Multi-Model Ensemble (NMME) project could have successfully predicted the recent epidemic at least 1–3 months in advance for several high-risk ZIKV zones, including its epicenter in Northeast Brazil (Muñoz et al., 2017, Epstein et al., 2017).

[1] International Research Institute for Climate and Society, Earth Institute, Columbia University, New York.

[2] Centre for the Mathematical Modelling of Infectious Diseases and Department of Infectious Disease Epidemiology, London School of Hygiene & Tropical Medicine, London.

[3] Department of Public Health and Preventive Medicine, Upstate Medical University, Syracuse, New York.

[4] WHO-WMO Joint Office for Climate and Health, WMO, Geneva.

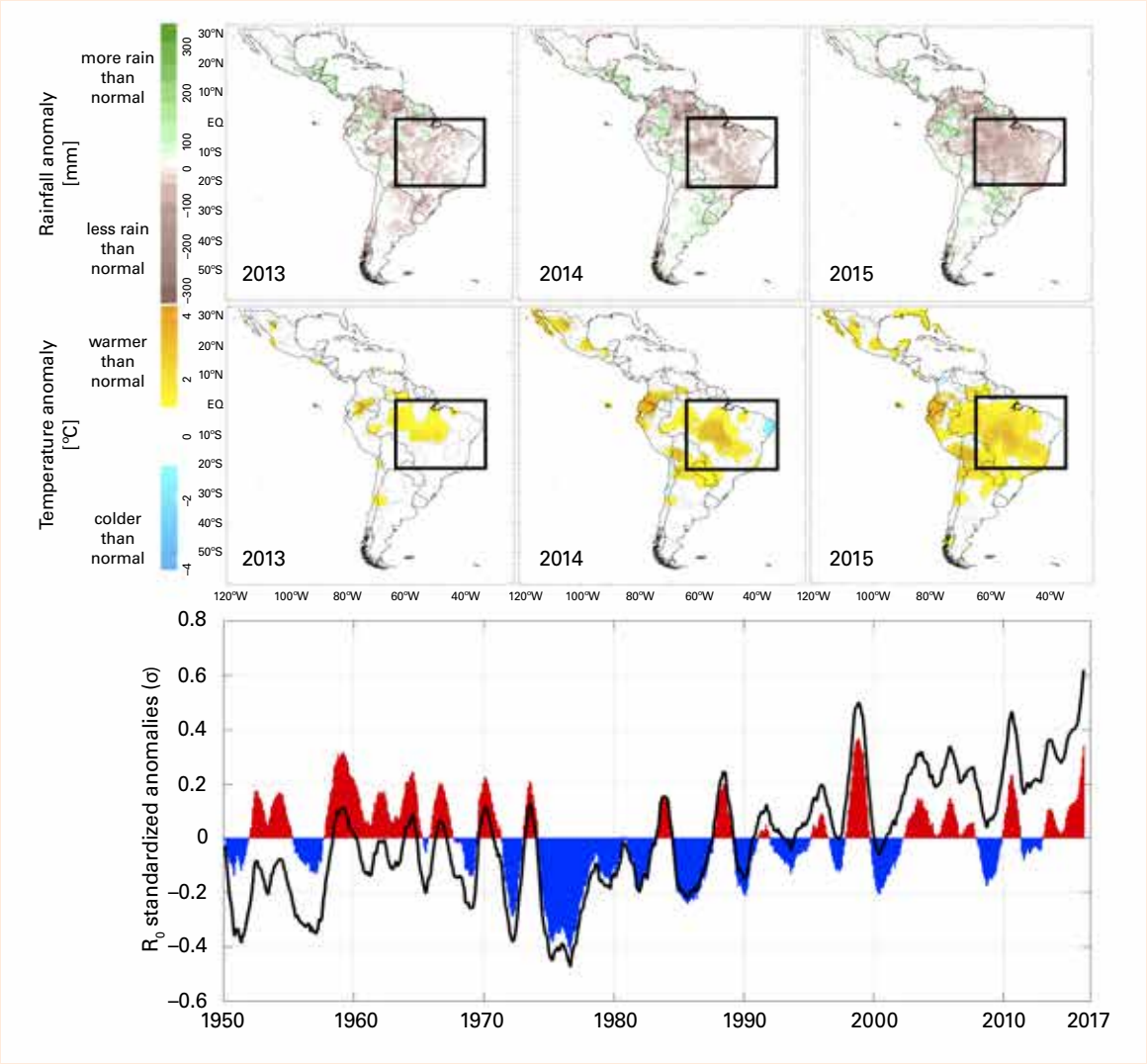

Annual rainfall anomalies (top panel) and temperature anomalies (middle panel) in 2013, 2014 and 2015; anomalies are computed with respect to the climatological period 1981–2010. Standardized anomalies of R_0 (bottom panel; units in standard deviations). The total potential risk of transmission (black curve) shows an upward trend consistent with climate warming and cannot be explained only by the contribution of El Niño and other year-to-year climate modes (filled curve): a combination of climate signals has been driving the risk of transmission in the region. Black boxes indicate the sector of analysis (After Muñoz et al., 2016*b*, 2017).

References

Epstein, H. et al., 2017: *A Menace Wrapped in a Protein: Zika and the Global Health Security Agenda*. New York, Columbia University, doi: 10.13140/RG.2.2.25050.85443.

Lowe, R. et al., 2018: The Zika virus epidemic in Brazil: From discovery to future implications. *International Journal of Environmental Research and Public Health*, 15(1): 96

Lowe, R. et al., 2014: Dengue outlook for the World Cup in Brazil: An early warning model framework driven by real-time seasonal climate forecasts. *The Lancet Infectious Diseases*, 14 (7): 619–626.

Lowe, R. et al., 2016: Evaluating probabilistic dengue risk forecasts from a prototype early warning system for Brazil. *eLIFE* 5:e11285.

Lowe, R. et al., 2017: Climate services for health: Predicting the evolution of the 2016 dengue season in Machala, Ecuador. *The Lancet Planetary Health* 1 (4):e142–e151.

Mordecai, E. A. et al., 2017: Detecting the impact of temperature on transmission of Zika, dengue, and chikungunya using mechanistic models. PLOS *Neglected Tropical Diseases*, 11(4):e0005568. doi: 10.1371/journal.pntd.0005568.

Muñoz, Á. G. et al., 2016*a*: *The Latin American and Caribbean Climate Landscape for ZIKV Transmission*. IRI Technical Report 2016-001. New York. doi: 10.7916/D8X34XHV.

Muñoz, Á. G. et al., 2016*b*: Analyzing climate variations at multiple timescales can guide Zika virus response measures. *Gigascience*, 5(1), 41.

Muñoz, Á. G. et al., 2017: Could the recent Zika epidemic have been predicted?' *Frontiers in Microbiology*, 8: 1291, https://www.frontiersin.org/articles/10.3389/fmicb.2017.01291/full.

Sorensen, C. J. et al., 2017: Climate variability, vulnerability, and natural disasters: A case study of Zika virus in Manabi, Ecuador following the 2016 earthquake. *GeoHealth*, 1(8):298–304, doi:10.1002/2017GH000104.

For more information, please contact:

World Meteorological Organization

7 bis, avenue de la Paix – P.O. Box 2300 – CH 1211 Geneva 2 – Switzerland

Communication and Public Affairs Office

Tel.: +41 (0) 22 730 83 14/15 – Fax: +41 (0) 22 730 80 27

Email: cpa@wmo.int

public.wmo.int

JN 18331